Th1 cytokine interferon gamma improves response in HER2 breast cancer by modulating the ubiquitin proteasomal pathway

Yongsheng Jia,[1,2,5] Krithika N. Kodumudi,[1] Ganesan Ramamoorthi,[1] Amrita Basu,[1] Colin Snyder,[1] Doris Wiener,[1] Shari Pilon-Thomas,[1] Payal Grover,[3] Hongtao Zhang,[3] Mark I. Greene,[3] Qianxing Mo,[4] Zhongsheng Tong,[5] Yong-Zi Chen,[6] Ricardo L.B. Costa,[2] Hyo Han,[2] Catherine Lee,[2] Hatem Soliman,[2] Jose R. Conejo-Garcia,[1] Gary Koski,[7] and Brian J. Czerniecki[1,2]

[1]Clinical Science & Immunology Program, H. Lee Moffitt Cancer Center, Tampa, FL, USA; [2]Department of Breast Oncology, H. Lee Moffitt Cancer Center, Tampa, FL, USA; [3]Department of Pathology and Laboratory Science, Perelman Medical School, University of Pennsylvania, Philadelphia, PA, USA; [4]Department of Biostatistics and Bioinformatics, H. Lee Moffitt Cancer Center, Tampa, FL, USA; [5]Department of Breast Oncology, National Clinical Research Center for Cancer, Key Laboratory of Breast Cancer Prevention and Therapy, Tianjin's Clinical Research Center for Cancer, Key Laboratory of Cancer Prevention and Therapy, Tianjin, China; [6]Department of Tumor Cell Biology, Key Laboratory of Cancer Prevention and Therapy, Tianjin's Clinical Research Center for Cancer, National Clinical Research Center for Cancer, Tianjin Medical University Cancer Institute and Hospital, Tianjin Medical University, Tianjin, China; [7]Department of Biologic Sciences, Kent State University, Kent OH, USA

HER2 breast cancer (BC) remains a significant problem in patients with locally advanced or metastatic BC. We investigated the relationship between T helper 1 (Th1) immune response and the proteasomal degradation pathway (PDP), in HER2-sensitive and -resistant cells. HER2 overexpression is partially maintained because E3 ubiquitin ligase Cullin5 (CUL5), which degrades HER2, is frequently mutated or underexpressed, while the client-protective co-chaperones cell division cycle 37 (Cdc37) and heat shock protein 90 (Hsp90) are increased translating to diminished survival. The Th1 cytokine interferon (IFN)-γ caused increased CUL5 expression and marked dissociation of both Cdc37 and Hsp90 from HER2, causing significant surface loss of HER2, diminished growth, and induction of tumor senescence. In HER2-resistant mammary carcinoma, either IFN-γ or Th1-polarizing anti-HER2 vaccination, when administered with anti-HER2 antibodies, demonstrated increased intratumor CUL5 expression, decreased surface HER2, and tumor senescence with significant therapeutic activity. IFN-γ synergized with multiple HER2-targeted agents to decrease surface HER2 expression, resulting in decreased tumor growth. These data suggest a novel function of IFN-γ that regulates HER2 through the PDP pathway and provides an opportunity to impact HER2 responses through anti-tumor immunity.

INTRODUCTION

HER2-positive (HER2^{pos}) breast cancer (BC) is an aggressive BC subtype associated with high relapse and mortality rates. In the past 30 years, with the development of HER2-targeted therapies, the survival of patients with HER2^{pos} BC has significantly improved. One standard of care approach for patients with locally advanced HER2^{pos} BC is neoadjuvant chemotherapy combined with the HER2-targeting agents trastuzumab and pertuzumab. The pathologic complete response (pCR) is a surrogate marker of long-term outcomes for overall survival (OS) for patients with BC, particularly with HER2^{pos} subtypes.[1,2] The immediate corollary to this observation is that improved pCR rate is a clinically valid endpoint not only for neoadjuvant clinical trials but also as a routine treatment goal. Notwithstanding the recent advances, nearly 50% of patients with HER2^{pos} BC still do not experience pCR after standard neoadjuvant systemic therapy. Patients with metastatic BC (MBC) inevitably acquire resistance to HER2-directed therapies, which highlights a need to develop treatments to overcome resistance.[3] Also vital is the need to combat central nervous system relapse.[4,5]

Accumulating data indicate that activation of immune pathways within the tumor predicts treatment efficacy and outcome in patients with HER2^{pos} BC.[6,7] We have previously shown that the anti-HER2 T helper 1 (Th1) response in the peripheral blood is a novel immune correlate to pCR following neoadjuvant trastuzumab and chemotherapy.[8] Therefore, combining HER2-targeted therapies with strategies to boost anti-HER2 Th1 immunity may improve outcomes and mitigate recurrence in high-risk patients.[8,9] The primary effectors of anti-tumor Th1 immunity, including interferon (IFN)-γ and tumor necrosis factor (TNF)-α, have been shown to decrease HER2 expression, reduce growth, induce senescence, and cause apoptosis in multiple HER2-expressing BC cells.[10–12]
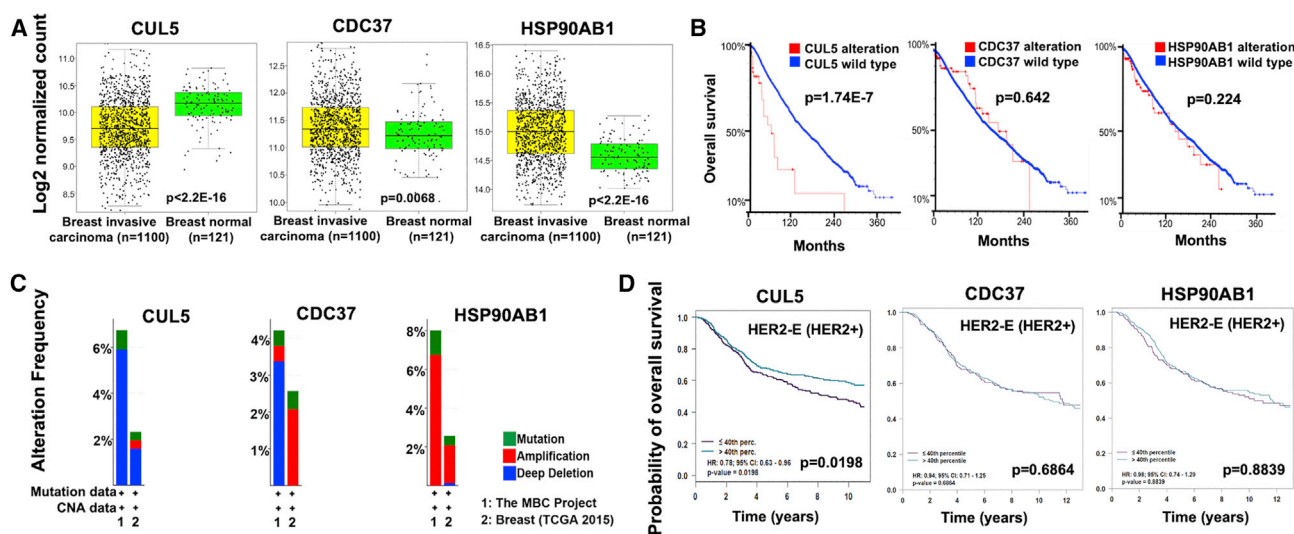
Figure 1. CUL5, CDC37, and HSP90AB1 expression in breast cancer

(A) CUL5, CDC37, and HSP90AB1 mRNA expression levels in invasive breast carcinoma patients and normal human breast tissues (CUL5, p < 2.2E−16; CDC37, p = 0.0068; HSP90AB1, p < 2.2E−16). (B) Overall survival in patients with CUL5 (p = 1.74E−7), CDC37 (p = 0.642), and HSP90AB1 (p = 0.224) mutation and wild type. (C) CUL5, CDC37, and HSP90AB1 gene alteration in early and metastasis breast cancer patient. (D) CUL5 (p = 0.0198), CDC37 (p = 0.6864), and HSP90AB1 (p = 0.8839) expression and survival in HER2-E/HER2pos (HER2-enriched) subtype breast cancer patients (cutoff at 40th percentile).

Generally, tyrosine kinase receptors following receptor activation are turned over by the proteasomal degradation pathway (PDP) and in the case of HER2 by the RING E3 ring ligase Cullin5 (CUL5). HER2 is protected from CUL5 degradation by binding with heat shock protein 90 (Hsp90). The specificity of Hsp90 client interactions is regulated by various co-chaperones, such as cell division cycle 37 protein (Cdc37), which has been shown to act as a co-chaperone in the interaction between Hsp90 and client proteins containing kinase domains.[13] The Cdc37-Hsp90 complex is a chaperone for HER2 and is thus an important regulator of the kinase.

The clinical reagent trastuzumab, an anti-HER2 monoclonal antibody, improves outcomes in women with early BC and MBC. Resistance to trastuzumab involves activation of the phosphatidylinositol 3-kinase (PI3K)/mammalian target of rapamycin (mTOR) pathway, overexpression of HER3 with increased heterodimerization, truncation of the HER2 extracellular domain, or lack of immune response.[14,15] The last decade has seen major advances in strategies to overcome resistance to trastuzumab. Therapeutic strategies used to overcome resistance to trastuzumab include the development of antibody-drug conjugates, novel anti-HER2 antibodies and bispecific antibodies, novel HER-directed tyrosine kinase inhibitors, dual HER2 inhibition strategies, and combinations with other drugs, including immunotherapy agents.[16] Currently, upon disease progression after treatment with HER2-targeted monoclonal antibodies, patients with HER2pos BC are treated with alternative targeted therapies, supporting the notion that HER2 is a predictive biomarker in heavily pretreated patients. In this setting, treatment with an oral tyrosine kinase inhibitor (lapatinib, neratinib, or tucatinib) or antibody drug conjugates (T-DM1 or DS8102a) have improved outcomes.[17–19]

In the present study we demonstrate a novel and clinically relevant pathway of HER2 regulation via the proteasome. First, we show that E3 ligase CUL5, when decreased or mutated, is associated with diminished OS in HER2 BC patients; second, we demonstrate that in both trastuzumab-resistant and -sensitive BC cells, IFN-γ enhances CUL5 expression and leads to dissociation of Cdc37 and Hsp90 from HER2, resulting in the latter's enhanced proteasomal degradation, diminished expression, and induction of senescence. Finally, we show that IFN-γ in combination with anti-HER2 antibodies dramatically reduces growth of both sensitive and resistant HER2-expressing BC and can overcome resistance to HER2-targeted therapies.

RESULTS

Reduced CUL5 expression predicts poor survival of BC patients

We first investigated the expression of proteins involved in the PDP of HER2. As shown in Figure 1A, CUL5 expression is significantly lower (p = 2.2E−16) in invasive BC (IBC) patients (n = 1,100) compared to healthy donors (n = 121), while the expression of co-chaperone proteins Hsp90 and Cdc37 protecting HER2 from degradation are elevated compared to normal breast tissue (Figure 1A). BC patients with CUL5 gene alteration demonstrate significantly impaired OS (p = 1.74E−7, Figure 1B), while there was no impact in survival seen with alterations in Hsp90 or Cdc37 expression (Figure 1B). Using the cBioPortal, CUL5 gene alteration was analyzed in MBC and early BC patients. BC samples (1,054 in total) from The Cancer Genome Atlas (TCGA) and the Metastatic Breast Cancer (MBC) project were used for mutation analysis for Figure 1C. The combined samples, including 817 TCGA samples and 237 MBC samples, were assayed by whole-exome sequencing along with matched normal pairs. As shown in
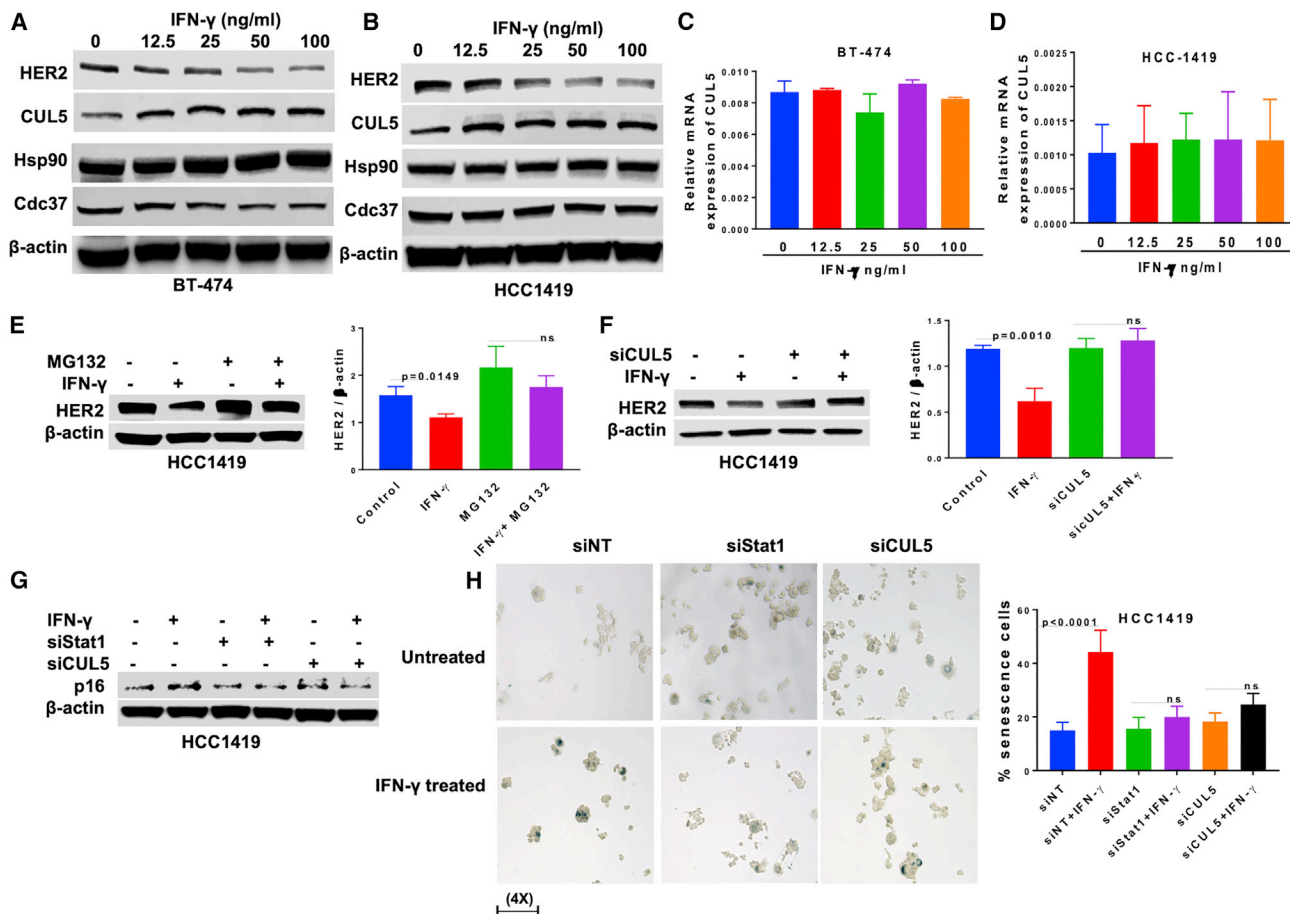
Figure 2. IFN-γ promotes CUL5-mediated HER2 degradation

(A and B) BT-474 (A) and HCC1419 (B) cells were treated for 96 h with increasing concentrations of IFN-γ (0, 12.5, 25, 50, and 100 ng/mL) and expression levels of HER2, CUL5, and HSP90 were detected by western blotting. (C and D) Relative mRNA expression of CUL5 in (C) BT-474 and (D) HCC1419 cells treated with increasing concentrations of IFN-γ for 48 h. (E) Proteasome inhibitor MG132 treatment for 2 h reverses IFN-γ-induced HER2 downregulation (p = 0.0149) in HCC1419 cells. (F) siCUL5 treatment reverses Th1 cytokine-induced HER2 downregulation (p = 0.0010) in HCC1419 cells. (G) IFN-γ induced p16 upregulation in HCC1419 cells following CUL5 or Stat1 siRNA transfection. (H) Silencing CUL5 or Stat1 interferes with IFN-γ-induced cell senescence in HCC1419 cells (siNT versus siNT+IFN-γ, p < 0.0001). Bar graphs represent % of SA-β-gal-positive cells, identified by ImageJ counting; mean ± SD (n = 3).

Figure 1C, there was CUL5 gene deletion in 2.33% of 817 invasive BC cases in TCGA data 2015 sets and in about 6.75% of 237 BC cases in the MBC project. Interestingly, there were also increased mutations in Cdc37 with gene alteration in 4.22% of 237 BC cases in the MBC project and gene alteration of 2.57% of 817 invasive BC cases in TCGA data 2015 (Figure 1C). We also observed Hsp90AB1 gene alteration in 8.02% of 237 BC cases in the MBC project, while we observed gene alteration with 2.57% of 817 cases in TCGA data 2015 (Figure 1C). Using the Breast Cancer Gene-Expression Miner v4.2 (bc-GenExMiner v4.2), we conducted CUL5 survival analysis in HER2^{pos} BC patients. Patients harboring tumors with low expression levels of CUL5 displayed a shorter survival compared to high CUL5-expressing tumors in the HER2^{pos} BC subtype (p = 0.0198, Figure 1D), but not in the estrogen receptor (ER)^{neg}HER2^{neg} BC subtype (p = 0.916, Figure S1A). We also observed significant correlation with CUL5 expression and OS in ER-

^{pos}/HER2^{neg} high proliferation (p = 0.0127, Figure S1A) and ER^{pos}/HER2^{neg} low proliferation (p = 0.0017, Figure S1A). For patients with HER2^{pos} BC, there was no relationship to survival for Hsp90 or Cdc37 expression (Figure 1D; Figures S1B and S1C). Altogether, the data suggest that diminished CUL5 gene expression is an independent negative prognostic factor in HER2^{pos} BC, which could promote tumor growth and survival in conjunction with increased Hsp90 and Cdc37 via protection of HER2 expression, leading to prolonged reflex signaling.

Effect of IFN-γ on CUL5 and co-chaperone proteins

To examine the effect of IFN-γ on co-chaperone proteins and HER2 expression, HER2-sensitive (BT-474) and -resistant cell lines (HCC1419) were treated with increasing concentrations of IFN-γ. We observed a dose-dependent decrease in HER2 expression (Figures 2A and 2B), with a concomitant increase in CUL5 protein levels.
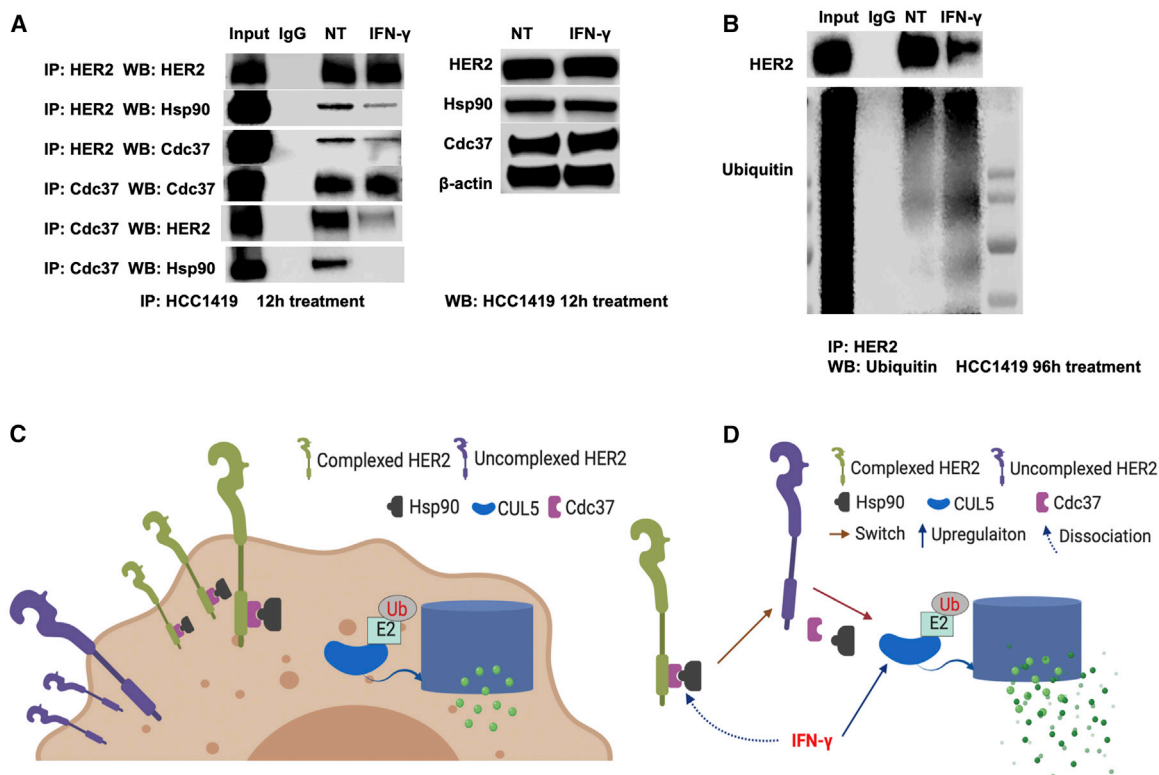
Figure 3. IFN-γ dissociates the HER2-Cdc37-HSP90 complex
(A) Immunoprecipitation of anti-HER2 or anti-CDC37 antibody followed by immunoblotting for HSP90 and HER2 in HCC1419 cells treated with IFN-γ for 12 h. (B) Immunoprecipitation with anti-HER2 antibody followed by western blotting showing increased ubiquitination of HER2 and decreased HER2 expression after treatment with IFN-γ for 96 h in HCC1419 cells. Input: 5 μg of input cell lysate. (C) Mode of complexed HER2 (HER2-Cdc37-HSP90) and uncomplexed HER2 in breast cancer cells. (D) Working mode of IFN-γ on HER2 downregulation via CUL5.

Interestingly, IFN-γ had a more substantial effect on HER2 downregulation in trastuzumab-resistant over trastuzumab-sensitive cells (Figure 2B; Figures S2A–S2E). IFN-γ did not increase the transcription of CUL5 as measured by quantitative real-time polymerase chain reaction (PCR) at different time points, suggesting that observed changes in CUL5 were due to post-transcriptional or translational effects of IFN-γ (Figures 2C and 2D; Figure S2F). IFN-γ-induced downregulation of HER2 was effectively blocked by proteasomal inhibitor MG132 treatment (Figure 2E, p = 0.0149). Similarly, knockdown of CUL5 (p = 0.0010) reversed the IFN-γ-induced HER2 downregulation in HCC1419 cells (Figure 2F).

Silencing CUL5 or Stat1 prevents senescence induced by IFN-γ
We then sought to determine whether CUL5 and STAT1 are necessary for Th1 cytokine-induced senescence in HER2^{pos} BC cells.[11] IFN-γ enhanced expression of the p16 senescence marker protein, but this upregulation was completely abrogated upon silencing of STAT1 or CUL5 in HCC1419 cells (Figures 2G and 2H) and other HER2-sensitive (SK-BR-3) and -resistant (MDA-MB-453 and JIMT-1) cells (Figure S3). Senescence associated β-galactosidase (SABG) activity in human HER2 BC cell lines further validated the

critical role of CUL5 in Th1 cytokine-induced cellular senescence. Indeed, the dramatic increase in 26%–29% of senescent cells, induced by Th1 cytokines, was completely abolished when STAT1 and CUL5 were silenced separately (Figure S4, p < 0.0001). These data suggest that induction of cellular senescence by IFN-γ is mediated through CUL5 and STAT1 signaling pathways.

Effect of IFN-γ on CUL5-mediated ubiquitination and degradation of HER2
Effect of IFN-γ on CUL5-mediated ubiquitination and degradation of HER2 was then evaluated in human HER2^{pos} BC cells. In HCC1419 cells, short-term IFN-γ treatment for 12 h resulted in reduced Hsp90 expression with intact HER2 level, suggesting reduced interaction between HER2 and Hsp90 and dissociation of the complex as a consequence of IFN-γ treatment (Figure 3A). Following IFN-γ treatment, coimmunoprecipitation with anti-Cdc37 antibody showed decreased expression of Hsp90, suggesting the effect of IFN-γ on Hsp90-Cdc37-mediated HER2 protection (Figure 3A). Immunoprecipitation (IP) with anti-HER2 antibody followed by immunoblotting showed that longer treatment (96 h) with IFN-γ resulted in ubiquitination of endogenous HER2
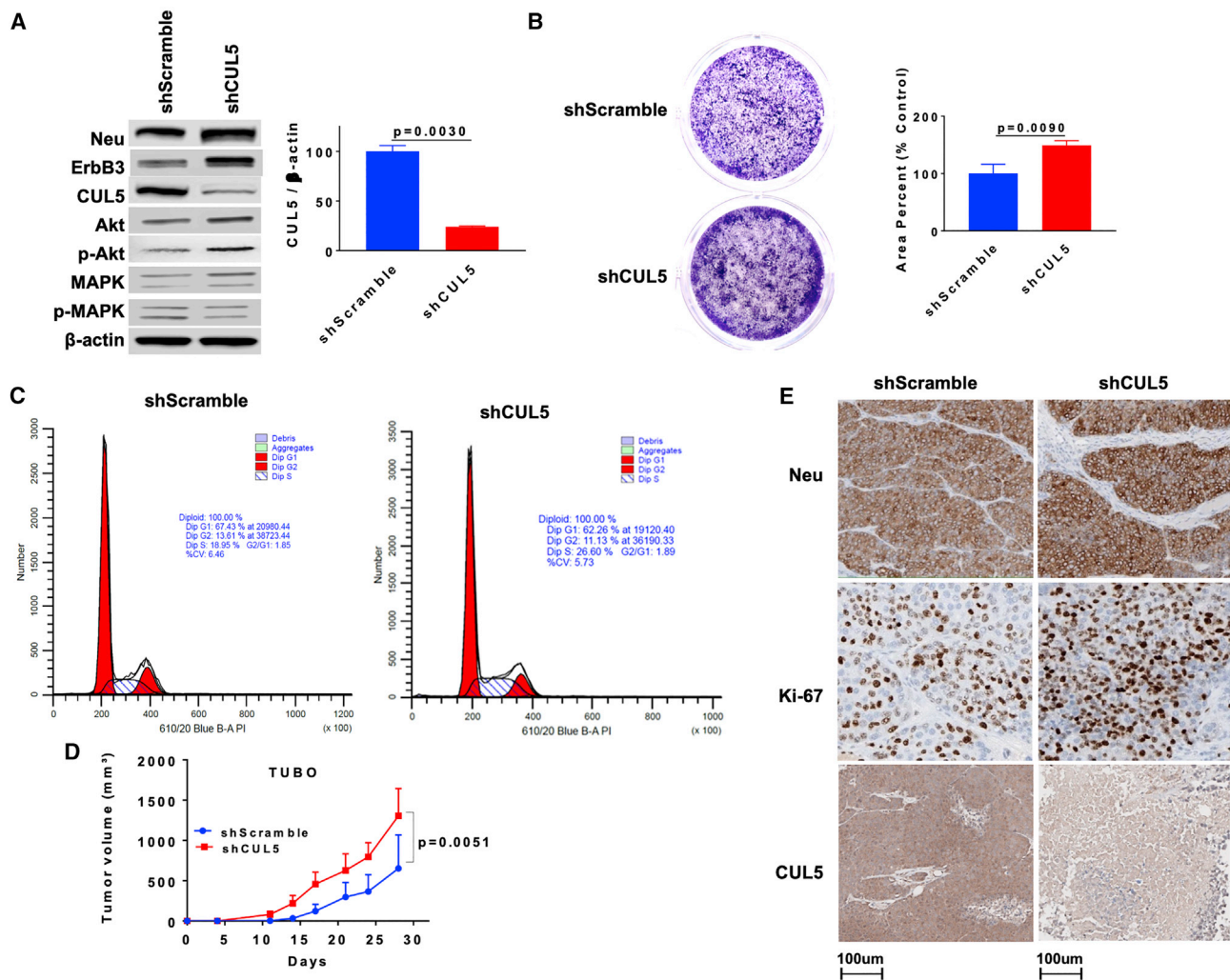
Figure 4. CUL5 knockdown promotes TUBO cells proliferation *in vitro* and *in vivo*

(A) Expression of neu, ErbB3, CUL5, HSP90, Akt, p-Akt, MAPK and p-MAPK in shScramble or shCUL5-transduced TUBO cells. (B) Analysis of cell proliferation by crystal violet proliferation assay showed higher proliferation after CUL5 knockdown in TUBO cells. Bar graphs represent % of control by crystal violet proliferation assay; shScramble versus shCUL5, p = 0.0090. (C) Analysis of cell cycle by flow cytometry showed increased accumulation of shCUL5-TUBO cells in S phase compared to shScramble-TUBO cells. (D) Orthotopic injection of shScramble and shCUL5 TUBO cells (3×10^4 cells, n = 8 per treatment group) resulted in faster tumor growth in shCUL5-TUBO mice, compared to shScramble controls (p = 0.0051). (E) Immunohistochemistry (IHC) analysis showed enhanced expression of neu and Ki-67 and reduced expression of CUL5 in tumors of shScramble and shCUL5-TUBO mice in shCUL5 versus shScramble tumors.

(Figure 3B). These data are consistent with downregulation of HER2 by IFN-γ being mediated via CUL5-induced ubiquitination and dissociation of Hsp90 from Cdc37 bound to HER2, leading to degradation of the HER2 receptor proteins. Figures 3C and 3D provide a working model of the impact of IFN-γ on the ubiquitination-proteasomal pathway. Based on our data, we propose that HER2-Cdc37-Hsp90 interaction in HER2^{pos} BC cells protect HER2 from the proteasomal degradation, induced by CUL5. Upon exposure to IFN-γ, this HER2-Cdc37-Hsp90 interaction is disrupted, leading to CUL5-mediated proteasomal degradation of HER2 and subsequent downregulation of pro-growth and survival signaling pathways.

Diminished CUL5 expression drives HER2 tumor progression

To investigate the role of CUL5 in HER2^{pos} BC, we used rat HER2 (neu) transgenic TUBO murine breast carcinoma cells. Knockdown of CUL5 in TUBO cells using lentiviral transduction resulted in substantially decreased (about 25% of control) CUL5 expression (Figure 4A). Notably, phosphorylation of AKT and mitogen-activated protein kinase (MAPK), proliferation activators downstream of ErbB receptors, were upregulated in CUL5 short hairpin RNA (shRNA) (shCUL5)-transduced TUBO cells, compared to Scramble shRNA (shScramble) controls (Figure 4A). To investigate the role of silencing CUL5 on cell cycle progression and proliferation in neu BC cells, cells were stained with crystal violet. As shown in Figure 4B,

shCUL5 TUBO cells led to increased proliferation of BC cells compared to shScramble TUBO cells. We observed an increase in the percentage of cells in the S phase upon CUL5 KD (18.95% versus 26.60% in shScramble versus shCUL5, Figure 4C), with a small decrease in the percentage of cells in the G_2-M phase, suggesting enhanced accumulation of cells in the synthesis phase and upregulated DNA replication. Next, we investigated the effect of CUL5 silencing in TUBO cell tumor growth. BALB/c mice were injected with shScramble or shCUL5 TUBO cells orthotopically at the mammary fat pad, and tumor growth was monitored twice a week. As shown in Figure 4D, shCUL5 tumor growth was significantly faster compared to shScramble controls in TUBO cell-bearing BALB/c mice (p = 0.0051). Immunohistochemistry (IHC) analysis of tumors from shCUL5 mice demonstrated greater neu and Ki-67 expression and reduced CUL5 expression compared to shScramble tumors (Figure 4E). Taken together, these data suggest that the degree of CUL5 expression can have a substantial impact on HER2^{pos} tumor growth and progression and suggest that the PDP pathway can modulate HER2 BC.

CUL5 and neu expression is regulated post-vaccination with neu-DC1

Using a neu peptide-loaded type I polarized dendritic cell (DC) vaccine, prior investigation in our laboratory has demonstrated the generation of an anti-neu Th1 immune response and therapeutic activity in the BALB/c neu TUBO cell models.[20] To examine the role of CUL5 in vivo in the neu-DC1 vaccination setting, we further tested the neu-DC1 vaccine for efficacy in BALB-neuT mice, an immunotolerant model that develop spontaneous BC as a consequence of mammary gland-specific expression of an activated HER2/neu oncogene.[21] As shown in Figure 5A, western blot analysis demonstrated downregulation of neu and upregulation of CUL5 in the tumors of neu-DC1 vaccinated mice. Neu T mice that received neu-DC1 vaccination demonstrated significantly delayed tumor growth compared to control (Figure 5B; p = 0.0003) and were sensitized to neu, as evidenced by enhanced IFN-γ production when re-stimulated in vivo with neu peptides, compared to splenocytes from control groups (Figure 5C, p < 0.0001). Downregulation of neu and upregulation of CUL5 were also confirmed by IHC (Figure 5D). Neu-DC1 efficacy was abrogated in the IFN-γ knockout (KO) mice, suggesting that the anti-tumor immune response was mediated by IFN-γ (Figure 5E). We observed accelerated tumor growth of shCUL5 tumors in wild-type BALB/c mice as shown in Figure 4D (p = 0.0051), while there was no difference in the tumor growth between shScramble or shCUL5 tumors in IFN-γ KO mice (Figure 5F). These data suggest that the antitumor effects of neu-DC1 vaccine are mediated through the Th1 cytokine IFN-γ, and that upregulation of CUL5 is needed for the IFN-γ-mediated anti-tumor immune response. It is noteworthy that we failed to observe any difference in neu and Ki-67 expression between the shScramble and shCUL5 knockdown in IFN-γ KO mice (Figure 5H). In addition, reduced CUL5 expression was observed in shCUL5 tumors compared to shScramble tumors in IFN-γ KO mice (Figure 5G). Taken together, these data suggest that CUL5-mediated neu downregulation is IFN-γ-dependent.

IFN-γ in combination with neu directed therapy in a murine BC model

Therapy-induced resistance to HER2-targeted agents remains a clinical problem in patients with HER2-driven cancers.[22,23] The TUBO neu mammary carcinoma displays all the characteristics of a trastuzumab-resistant cell (Figure 6A). As shown in Figure 6A, treatment of neu^{pos} TUBO cells with anti-neu monoclonal antibodies (anti-neu antibodies 7.16.4 and 7.9.5 that mimic trastuzumab and pertuzumab)[12] demonstrate that these cells are relatively resistant to the neu-blocking antibodies. However, addition of IFN-γ significantly induced proliferation arrest in TUBO cells compared to monotherapy (Figures 6A and 6B). We also observed synergy in cell proliferation inhibition with the commonly used chemotherapeutic drug paclitaxel and IFN-γ (Figures 6A and 6B). The observed synergy, however, was not as effective as IFN-γ and anti-neu combination (Figures 6A and 6B). No significant synergistic effect on proliferation arrest was noted in TUBO cells when paclitaxel was added to IFN-γ and neu combination (Figures 6A and 6B). In addition, IP with anti-neu antibody followed by western blot analysis revealed that IFN-γ + anti-neu (anti-neu antibodies 7.16.4 and 7.9.5) combination downregulated neu in TUBO cells through proteasomal degradation (Figure 6C). Since we observed the synergistic effect of IFN-γ in combination with neu-targeted therapy and paclitaxel in inhibiting cellular proliferation and downregulation of neu via proteasomal degradation, we examined this combinatorial effect in vivo in preclinical mammary tumor models. As shown in Figure 6D (p = 0.0263), IFN-γ administered systemically in combination with anti-neu antibody significantly delayed tumor growth compared to monotherapy. In addition, neu-DC1 administered in combination with anti-neu (anti-neu clones 7.16.4 and 7.9.5) antibodies significantly induced tumor regression (Figure 6E) and enhanced survival (Figure 6F). In addition, we observed downregulation of neu surface expression in tumors of mice that received combination therapy with IFN-γ and anti-neu antibody compared to IFN-γ or anti-neu antibodies alone (Figure 7A). Furthermore, IFN-γ in combination anti-neu antibody blockade increased the percentage of senescent cells as shown in Figures 7B and 7C, compared to IFN-γ alone (p = 0.0072). In addition, in vivo tumors of mice treated with neu-DC1 and murine anti-neu antibodies demonstrated significant downregulation of neu surface expression compared to the untreated control group or monotherapy as analyzed by IHC (p = 0.0001) (Figure 7D). These data suggest that the Th1 immune response with neu-targeted therapy in neu-resistant cells has at least an additive effect in downregulating neu, inducing tumor senescence and mediating tumor regression in a preclinical model of neu[pos] BC.

IFN-γ treatment reverses resistance to HER2-targeted agents

Since IFN-γ and trastuzumab and pertuzumab impact HER2 expression through different mechanisms we tested whether combinations can synergize or have additive effects in trastuzumab-sensitive (SKBR3 and BT-474) and -resistant (HCC1419 and JIMT-1) cells.

We examined the dose-dependent effect of trastuzumab and IFN-γ. As expected (Figure 8A), HER2-sensitive BC cells (SK-BR-3 and
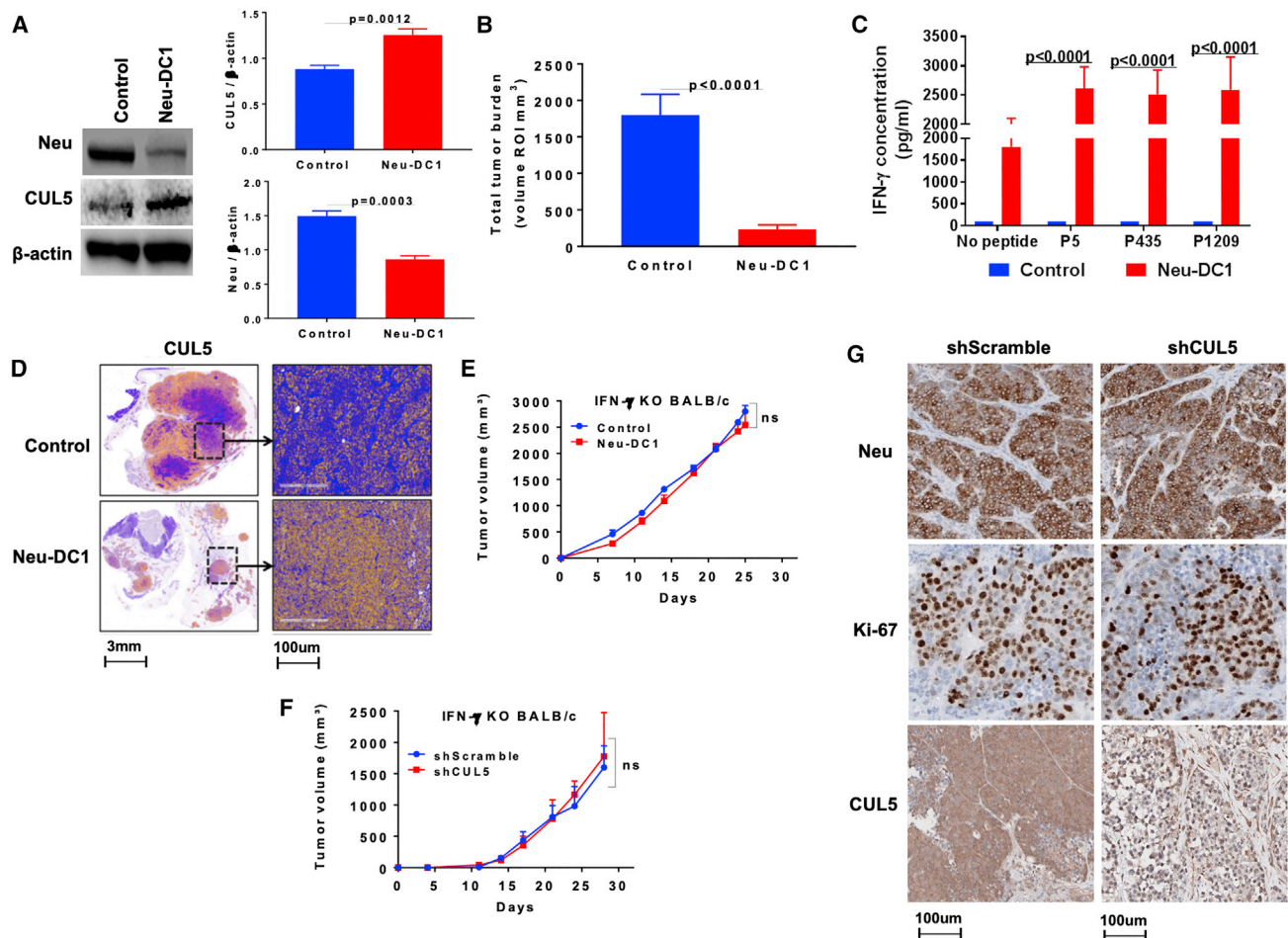
Figure 5. CUL5 and HER2 expression levels are dependent on IFN-γ

(A) Expression of neu and CUL5 were detected by western blotting in control and DC vaccine-treated NeuT murine tumor samples (n = 3). (B) Tumor growth in BALB-HER2/neu transgenic mice (neu T) treated with neu-DC1 vaccine, compared to control mice at 16 weeks of age. Spontaneous tumor growth in mammary glands was monitored by MRI (p < 0.0001). (C) Significantly increased IFN-γ secretion by splenocytes isolated from neu-DC1-vaccinated BALB-HER2/neuT mice, when re-stimulated with 2 µg/mL class II neu peptides (P5, P435, and P1209) for 72 h and measured by IFN-γ ELISA in culture supernatants (n = 3). (D) IHC analysis of CUL5 expression in BALB-HER2/neu transgenic mice after neu-DC1 treatment. (E) Anti-tumor effect of neu-DC1 is reversed in IFN-γ knockout mice bearing TUBO tumors (n = 8 per treatment group), TUBO cells (3×10^4) were orthotopically injected into mammary fat pad (n = 8 per treatment group). shScramble and shCUL5 TUBO cells (3×10^4) were orthotopically inoculated into (F) IFN-γ knockout mice. n = 8 per treatment group. (G) IHC analysis of neu, Ki-67, and CUL5 expression in shScramble and shCUL5 tumor tissues from IFN-γ knockout mice (n = 8 per treatment group).

BT-474) were sensitive to trastuzumab treatment while HER2-resistant cells (JIMT-1 and HCC1419) were relatively resistant to trastuzumab. Murine HER2^{pos} TUBO cells were significantly resistant to anti-neu antibody 7.16.4 (which mimics trastuzumab, Figure 8A). When resistant cells were treated with IFN-γ, even the lowest concentration of IFN-γ was highly effective in inhibiting the proliferation of trastuzumab-resistant cell lines compared to trastuzumab-sensitive cells (Figure 8B). These data provided a rationale to combine IFN-γ with anti-HER2-targeted therapies. To test this, HER2- sensitive and -resistant cells were treated with IFN-γ, alone and in combination with trastuzumab plus pertuzumab (T+P). We observed synergy in proliferation arrest in both HER2-sensitive SK-BR-3 cells (Figure 8C; control versus IFN-γ plus T+P [I+T+P], p < 0.0001; IFN-γ

versus I+T+P, p = 0.0009, T+P versus I+T+P, p = 0.0345) and HER2-resistant HCC1419 cells (Figure 8D; control versus I+T+P p < 0.0001; IFN-γ versus I+T+P, p = 0.0134; T+P versus I+T+P, p < 0.0001) when IFN-γ was combined with T+P. We pre-treated the human HER2-expressing cell line JIMT-1 (also resistant to trastuzumab) with or without IFN-γ or T+P *in vitro* for 48 h. Viable cells from each group were injected in non-obese diabetic (NOD)/severe combined immunodeficiency (SCID)-γ$^{-/-}$ (NSG) mice. In mice that are injected with IFN-γ-treated JIMT-1 cells, we observed significant delay in tumor growth compared to other groups (p = 0.052) (Figure 8E). We next investigated the effect of IFN-γ in combination with anti-HER2 agents on HER2 ubiquitination. IP with anti-HER2 antibody followed by western blot analysis revealed that I+T+P
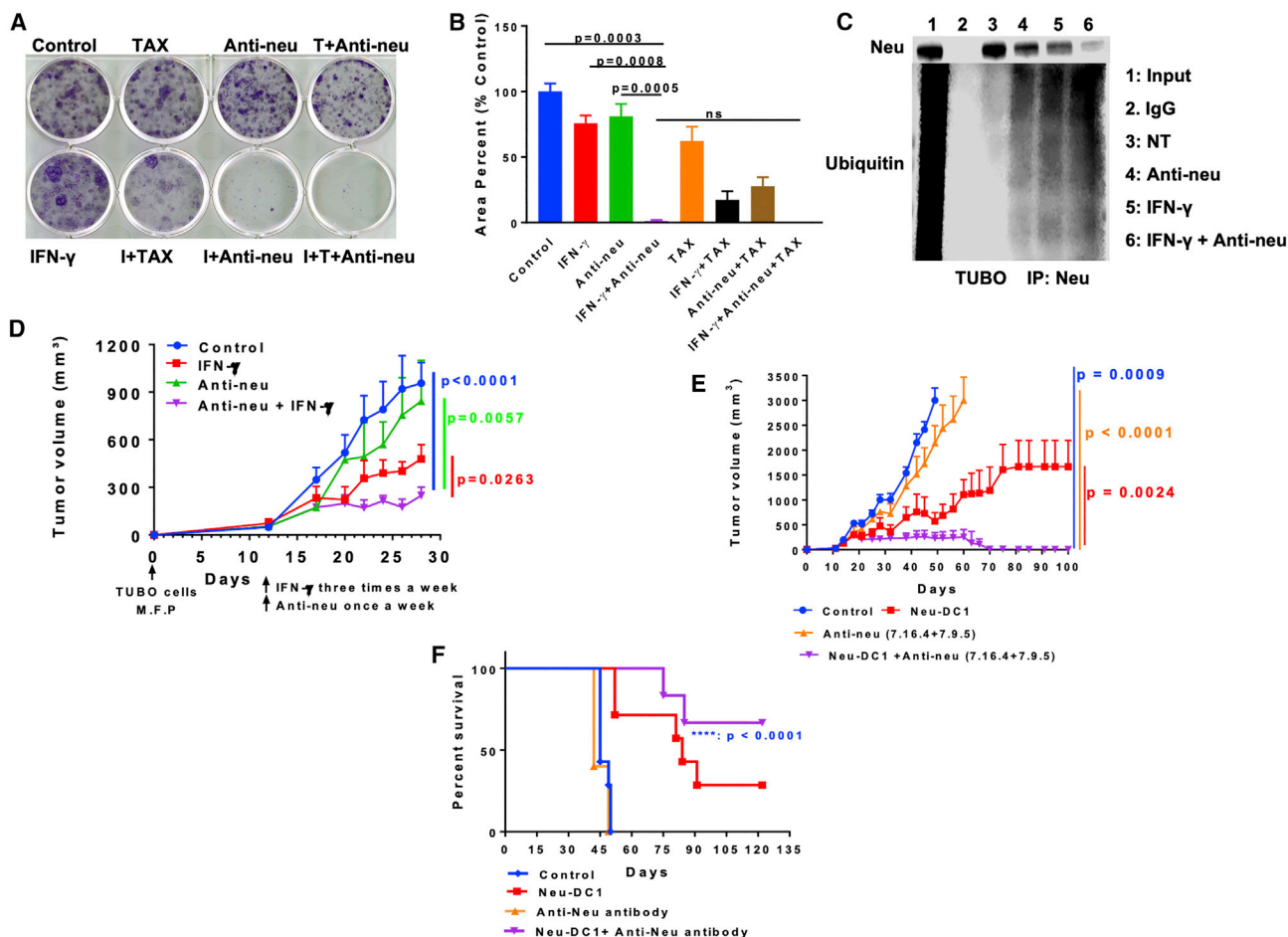
Figure 6. Effect of IFN-γ, anti-neu, and paclitaxel combination therapy on TUBO cells and tumor growth in TUBO-bearing mice

(A) Combination treatment with IFN-γ (0.1 ng/mL) and murine anti-neu antibodies (7.16.4, 5 μg/mL; 7.9.5, 5 μg/mL) or paclitaxel (2 nM) for 6 days induced proliferation arrest in TUBO cells (mean ± SD; n = 3). (B) Bar graphs represent % of control by crystal violet proliferation assay: control versus IFN-γ+anti-neu (p < 0.0001), anti-neu versus IFN-γ+anti-neu (p < 0.0001), and IFN-γ versus IFN-γ+anti-neu (p < 0.0001). (C) Immunoprecipitation with Anti-neu antibody followed by western blotting showing decreased neu expression and increased ubiquitination of the receptor protein after treatment with IFN-γ, anti-neu, and IFN-γ+anti-neu for 48 h in TUBO cells. Input: 5 μg of input cell lysate. (D) Tumor growth curve in TUBO mice that were treated with IFN-γ (intraperitoneal 5×10^5 IU/kg, three times weekly), murine anti-neu antibodies (clone 7.16.4, 50 μg; 7.9.5, 50 μg; intraperitoneal, weekly once) and a combination of IFN-γ and anti-neu antibodies, starting on day 12 after tumor inoculation (control versus IFN-γ+anti-neu, ***p < 0.0001; anti-neu versus IFN-γ+anti-neu, **p = 0.0057; IFN-γ versus IFN-γ+anti-neu, *p = 0.0263). (E) Tumor growth in TUBO mice treated with neu-DC1 intratumorally once a week for 6 weeks, murine anti-neu antibodies (clone 7.16.4, 50 μg; 7.9.5, 50 μg; intraperitoneal, weekly once), and a combination of neu-DC1 and anti-neu antibodies, starting on day 12 after tumor inoculation (control versus IFN-γ+anti-neu, ***p < 0.0001; anti-neu versus IFN-γ+anti-neu, **p = 0.0057; IFN-γ versus IFN-γ+anti-neu, *p = 0.0263). (F) Survival curve.

combination downregulated HER2 through ubiquitination degradation even further compared to T+P or IFN-γ alone in SKBR-3 cells (Figure 9A). In addition, I+T+P significantly increased CUL5 and decreased Cdc37 at total protein levels (Figure 9B). In HER2-resistant HCC1419 cells, combination with I+T+P resulted in similar downregulation and ubiquitination of HER2 (Figure 9C), reduced Cdc37 levels (Figure 9D), as well as decreased surface HER2 expression, while there was no change in CUL5 expression (Figure 9D). In addition, we observed reduced HER2 expression in HCC1419 cells when treated with I+T+P compared to single treatment alone (Figure 9E). Based on these results, we provide a working model of the impact

of combining IFN-γ with trastuzumab and pertuzumab on the ubiquitination-proteasomal pathway. We propose that trastuzumab and pertuzumab combination treatment leads to proteasomal degradation of free uncomplexed HER2 by downregulation of Cdc37 while IFN-γ interferes with the HER2-Cdc37-Hsp90 complex, leading to CUL5-mediated proteasomal degradation of HER2 (Figure 9F).

Anti-HER2 antibodies, trastuzumab, and pertuzumab have been shown to cause regression of HER2^{pos} tumors[24] in at least some patients and downregulate HER2 expression in BC.[25,26] The mechanism by which combination HER2 antibodies downregulate HER2
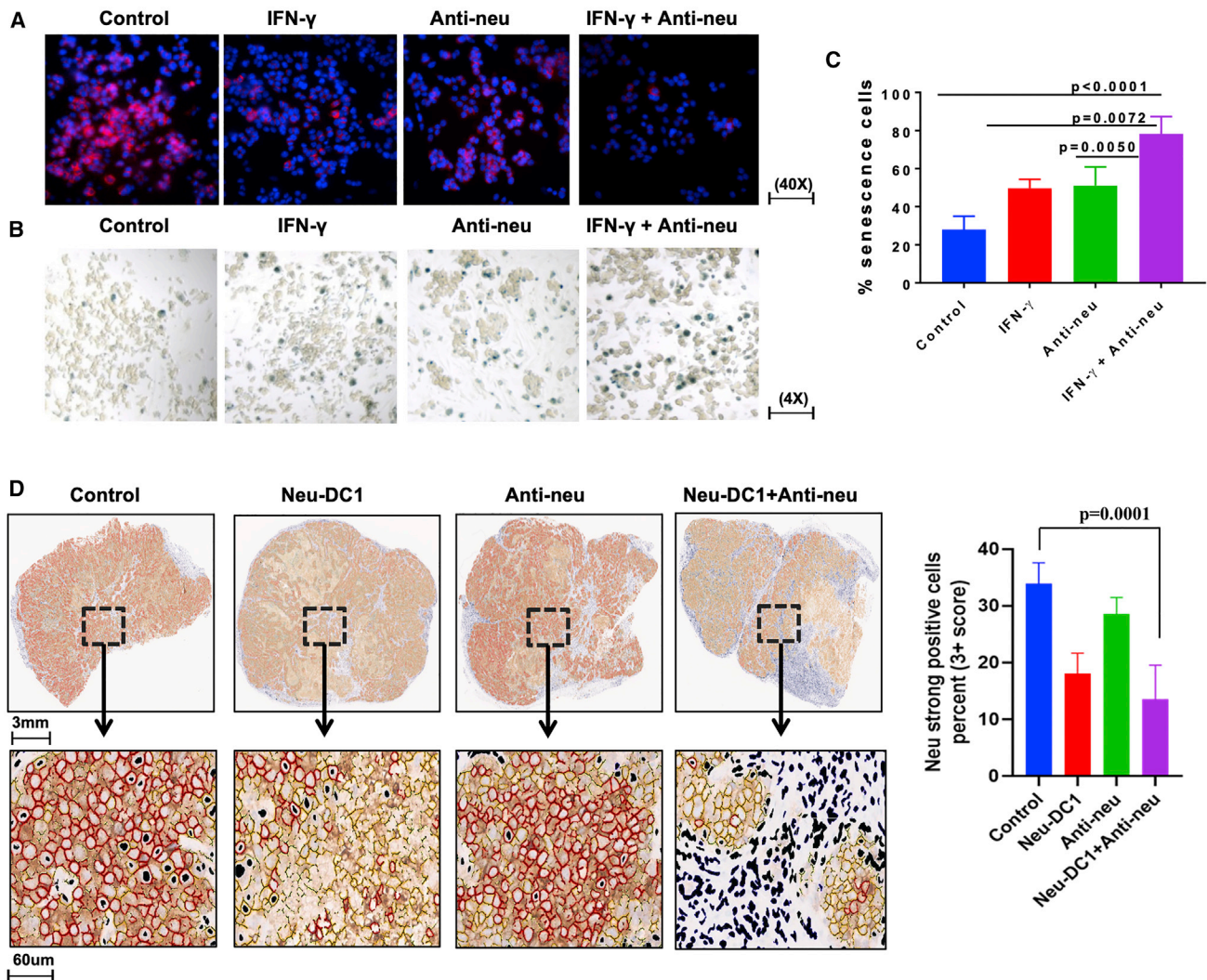
Figure 7. Synergistic effect of anti-neu and IFN-γ on neu downregulation in TUBO cells

(A) Neu expression in *ex vivo* tumors of mice treated with IFN-γ, anti-neu alone, or IFN-γ and anti-neu in combination by immunofluorescence as specified (red, neu; blue, nuclear, DAPI). (B) Senescence in *ex vivo* tumor cells isolated from control and treated mice by a SABG assay. (C) Bar graphs represent % of SA-β-gal-positive cells by ImageJ counting; mean ± SD (n = 3) (control versus IFN-γ+anti-neu, $p < 0.0001$; anti-neu versus IFN-γ+anti-neu, $p = 0.0050$; IFN-γ versus IFN-γ+anti-neu, $p = 0.0072$). (D) Immunohistochemistry analysis of neu surface expression on *in vivo* tumors.

expression is not entirely clear. Hence, we investigated whether the anti-HER2 antibodies can impact the PDP specifically with either CUL5 or the protective protein complex Cdc37-Hsp90. We treated HER2-resistant and -sensitive BC cells with trastuzumab (T), pertuzumab (P), or a combination of both (T+P). As shown in Figure S5A, we observed membrane-bound expression of HER2 and Cdc37 in BT-474 cells as analyzed using confocal microscopy. HER2-sensitive (BT-474 and SK-BR-3) and -resistant cells (TUBO) treated with both anti-HER2/neu antibodies (T+P or anti-neu 7.16.4 and 7.9.5) display significant downregulation of HER2 as well as a modest decrease in chaperone protein Cdc37 compared to untreated trastuzumab and pertuzumab alone, while there was no effect on CUL5 and Hsp90 (Figure S5B). In addition, T+P treatment resulted in ubiquitination

of endogenous HER2 and degradation of HER2 receptor proteins compared to trastuzumab or pertuzumab alone, in both sensitive and resistant cells (Figure S5C). Since we observed downregulation of co-chaperone, Cdc37 with T+P, we examined the association of the HER2-Hsp90-Cdc37 complex. While trastuzumab or pertuzumab alone did not alter Hsp90 protein level, T+P resulted in a significant increase in Hsp90 and Cdc37 being complexed with HER2, protecting HER2 from degradation (Figure S5D). Based on these results, we propose that trastuzumab and pertuzumab combination treatment leads to proteasomal degradation of free uncomplexed HER2 by downregulation of Cdc37, but there is also a paradoxical increase in the Cdc37-Hsp90-HER2 complex that forms, protecting HER2 from further degradation (Figures S5E and S5F) by E3 ligases. These data suggest
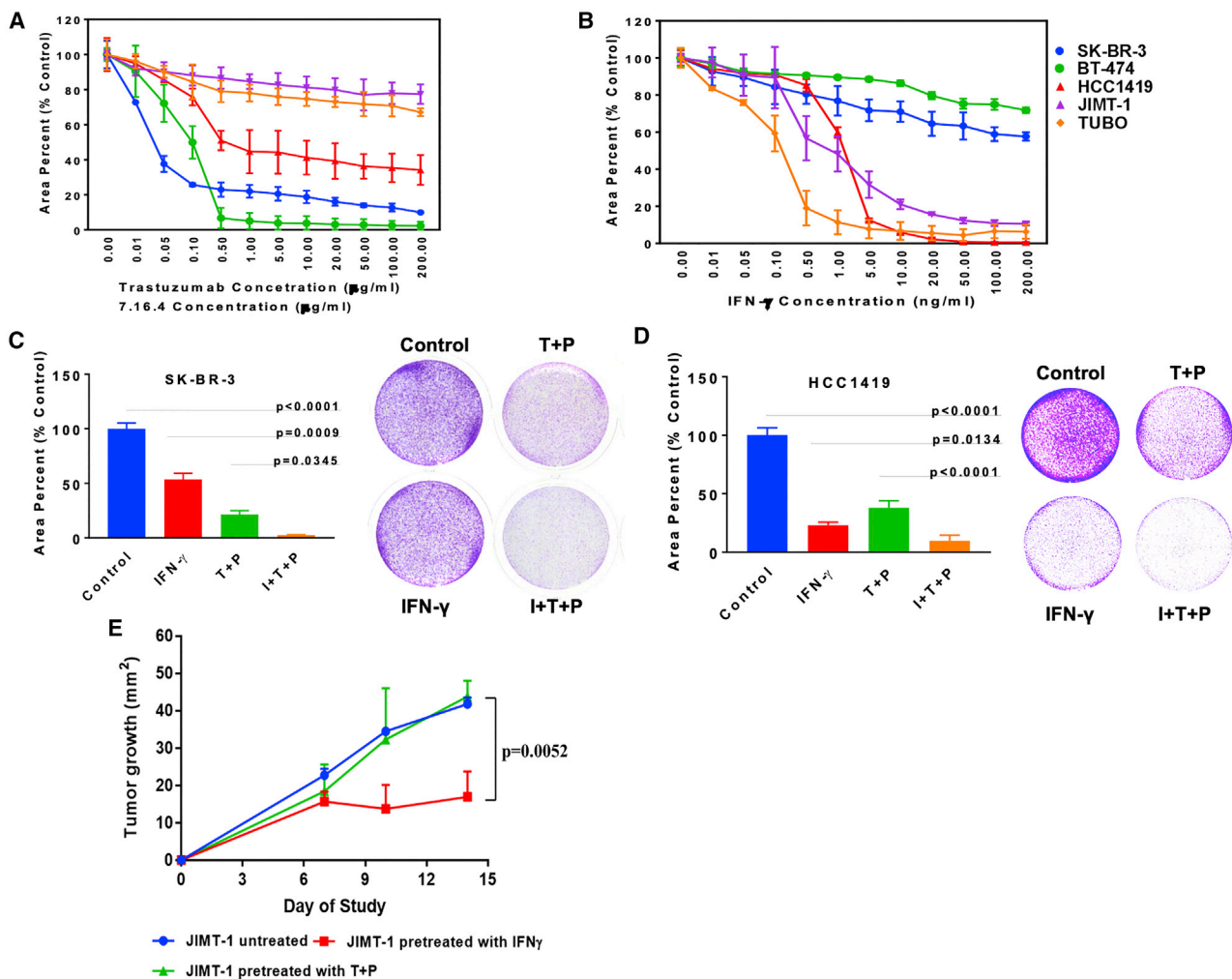
Figure 8. IFN-γ treatment reverses resistance to trastuzumab and pertuzumab therapies

(A–C) Trastuzumab-sensitive cell lines SK-BR-3 and BT-474 and trastuzumab-resistant cell lines HCC1419 and JIMT-1 and TUBO murine breast carcinoma cells were treated with different concentrations of (A) trastuzumab (0–200 μg/mL), anti-neu antibody clone 7.16.4 (0–200 μg/mL) in TUBO cells; (B) IFN-γ (0–200 ng/mL); and (C) the trastuzumab-sensitive cell line SK-BR-3 was treated with IFN-γ and T+P for 6 days, followed by crystal violet proliferation assay. Control versus I+T+P, p < 0.0001; IFN-γ versus I+T+P, p = 0.0009; T+P versus I+T+P, p = 0.0345. T+P, trastuzumab (0.5 μg/mL) + pertuzumab (0.5 μg/mL); IFN-γ, 50 ng/mL (n = 3). (D) Treatment with IFN-γ and T+P for 6 days inhibits cellular proliferation in HCC1419 cells, which are primarily resistant to trastuzumab. Control versus I+T+P, p < 0.0001; I versus I+T+P, p = 0.0134; T+P versus I+T+P, p < 0.0001. T+P, trastuzumab (10 μg/mL) + pertuzumab (10 μg/mL); IFN-γ, 10 ng/mL (n = 3). (E) The trastuzumab-resistant cell line JIMT-1 was treated with or without IFN-γ (10 ng/mL) or T+P (5 μg/mL each) for 48 h *in vitro*. Equal numbers of viable cells from each group were collected and injected in NSG mice subcutaneously. Tumor growth was measured twice a week.

that the PDP Cdc37-Hsp90 complex plays a critical role in HER2 overexpression and ultimately cell signaling mediated by HER2, and trastuzumab and pertuzumab may impact HER2^{pos} BC at least in part by this pathway.

Lastly, we investigated the effect of IFN-γ in combination with other HER2 targeted agents, lapatinib and T-DM1. HER2-sensitive and -resistant cells were treated with IFN-γ alone and in combination with lapatinib and T-DM1. Synergistic proliferation arrest was noted in these cell lines when IFN-γ was combined with lapatinib and T-DM1 (Figures S6A–S6D). These data demonstrate that addition of

IFN-γ can overcome resistance to HER2-targeted therapies. Our data suggest that addition of IFN-γ further enhanced the loss of proliferation in resistant HER2^{pos} BC cells. These anti-HER2-targeted agents alone did not induce proliferation arrest in ER[pos]/HER2^{neg} cell lines MCF-7 and T47D (Figures S7A and S7B), suggesting that the effect of IFN-γ observed in our study is specific for HER2^{pos} BC.

DISCUSSION

Our data demonstrate the existence of a novel pathway of immune control over HER2-expressing tumors. We show that the ubiquitination-proteasomal pathway plays a substantial role in maintaining
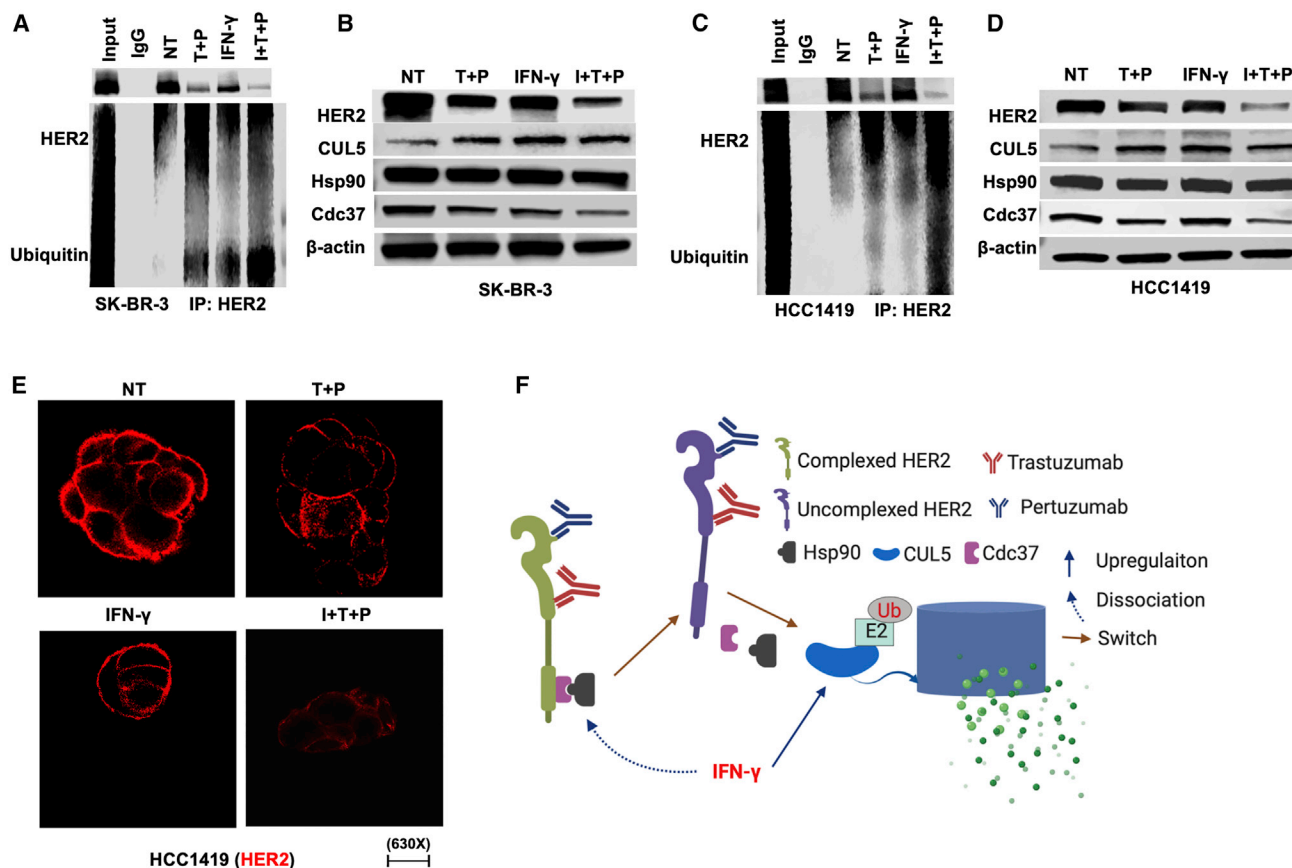
Figure 9. IFN-γ treatment enhances trastuzumab- and pertuzumab-induced HER2 degradation

(A) Immunoprecipitation with anti-HER2 antibody in SKBR3 cells. (B) Western blot analysis after treatment with IFN-γ, T+P, and I+T+P in SKBR3 cells. (C) Immunoprecipitation with anti-HER2 antibody in HCC1419 cells. (D) Western blot analysis after treatment with IFN-γ, T+P, and I+T+P in HCC1419 cells. (E) Confocal microscopy showed reduced HER2 expression after treatment with T+P, IFN-γ, and IFN-γ and T+P for 48 h in HCC1419 cells. T+P, trastuzumab (10 μg/mL) + pertuzumab (10 μg/mL); IFN-γ, 10 ng/mL. (F) Working mode of IFN-γ plus trastuzumab and pertuzumab therapy induces HER2 downregulation via the proteasomal degradation pathway.

HER2 expression in HER2^{pos} and luminal BCs, with lower expression being associated with poor survival. While HER2-targeted therapies have dramatically improved survival in HER2^{pos} BC, those with locally advanced or metastatic disease often become refractory or resistant to HER2-directed therapies.[27] In this study, we provide evidence that the Th1 immune response, mediated primarily through IFN-γ, can enhance the activity of all HER2-targeted agents tested in both sensitive and resistant BC cells. This study provides a crucial link between Th1 immunity and HER2-mediated responses, offering a novel opportunity to add to the armamentarium directed against HER2^{pos} cancers. It has been previously demonstrated that increasing infiltrating lymphocytes showed significant correlation with increased odds of pCR as well as long-term survival in HER2^{pos} BC.[28,29] This study delineates a mechanism through which IFN-γ can increase the activity of the ubiquitin-proteasomal pathway leading to breakdown of HER2 from the cell surface, leading to apoptosis and induction of tumor senescence. When combined with HER2-targeted therapies, IFN-γ can further promote proliferation arrest and reduction in tumor growth.

Currently, most of the HER2-directed therapies require relatively intense chemotherapy or have chemotherapy molecules conjugated to antibodies such as T-DM1 and DS-8201a.[30] The chemotherapy given systemically with HER2-directed therapies has significant associated toxicities. This study suggests that low doses of IFN-γ or vaccines activating the anti-HER2 CD4 Th1 response can have a significant effect on HER2 tumor growth when used in conjunction with HER2-directed therapies. Even those resistant to antibody conjugates such as T-DM1 can be improved when combined with IFN-γ, suggesting that combining Th1 immune therapies can effectively reduce the concentration and enhance the effectiveness of all HER2-directed therapies. We have initiated a phase 2 clinical trial adding low-dose systemic IFN-γ with weekly paclitaxel, trastuzumab, and pertuzumab in locally advanced-stage hormone receptor-positive ER^{pos}HER2^{pos} BCs in the neoadjuvant setting, since these patients do not display similar high pCRs than ER^{neg}HER2^{pos} BC (ClinicalTrials.gov: NCT03112590).

Cells resistant to HER2-targeted agents were particularly more sensitive to the growth arrest and senescence induction caused by IFN-γ

compared with those that were sensitive. Thus, increasing anti-HER2 CD4 Th1 responses may be especially beneficial in patients who become refractory to HER2-directed therapy regimens. As such, Th1 immunity through IFN-γ may offer an alternative immune approach to treat HER2 resistance, with even sensitive tumors possibly benefiting from combining IFN-γ with HER2-directed therapies. Interestingly, HER2 tumors have not been particularly sensitive to checkpoint therapy,[31] but since IFN-γ drives antigen presentation and PD1 expression on T cells it may make HER2 BC more sensitive to checkpoint therapy as well.

The mechanism by which trastuzumab and pertuzumab increase pCR and survival in HER2 BC has not been clearly defined. It has been proposed that pertuzumab interferes with HER2-HER3 dimerization, leading to decreased proliferation.[25,32] Interestingly, in the current study it is clear that dual trastuzumab and pertuzumab, compared to individual antibody, leads to diminished expression of the linker protein Cdc37, and there was increased ubiquitination of HER2; however, we noted a paradoxical increase in HER2 association with Cdc37 and Hsp90, suggesting a protective mechanism that combination anti-HER2 therapy may also cause. Interestingly, this can be combatted by IFN-γ that caused the dissociation of HER2 from Cdc37 and Hsp90, suggesting the synergy that exists between Th1 immunity and anti-HER2 therapies.

IFN-γ or Th1 immunity may not be very effective by itself in treating HER2 cancers, but when combined with anti-HER2 therapy it could be extremely potent. Differences in anti-HER2 Th1 immunity may account for the decreased sensitivity to HER2-targeted agents that are observed in HER2^{pos} cancers other than BC. This study demonstrates a unique mechanism by which the immune response can cooperate with HER2-targeted agents to enhance activity in HER2 cancer therapy. Our data indicate the existence of a novel pathway that interplays between the humoral and cellular immune response in the elimination of HER2-expressing cancers. The cellular immune response through IFN-γ mobilizes the proteasomal pathway activation leading to HER2 degradation when combined with HER2-targeted agents, improving the therapeutic effectiveness in both trastuzumab-sensitive and -resistant cells and offering a novel approach to the treatment of HER2-expressing cancers.

MATERIALS AND METHODS
Cell culture and treatments
Human BC cell lines BT-474, ZR-75-30, MDA-MB-361, SK-BR-3, MDA-MB-453, and HCC1419 were obtained from the American Type Culture Collection (Manassas, VA, USA) and grown in complete media (CM) consisting of RPMI 1640 (Life Technologies, Grand Island, NY, USA) supplemented with 10% heat-inactivated fetal bovine serum (FBS, Cellgro, Herndon, VA, USA), 0.1 mM nonessential amino acids, 1 mM sodium pyruvate, 2 mM fresh L-glutamine, 100 mg/mL streptomycin, 100 U/mL penicillin, 50 mg/mL gentamycin, 0.5 mg/mL Fungizone (all purchased from Life Technologies, Rockville, MD, USA), and 0.05 mM 2-mercaptoethanol (2-ME) (Sigma-Aldrich, St. Louis, MO, USA). The JIMT-1 cell line was purchased from DSMZ (Braunschweig, Germany) and were grown in

Dulbecco's modified Eagle's medium (DMEM) (Invitrogen, Waltham, MA, USA) supplemented with 10% FBS. The TUBO BC cell line (kind gift from Dr. Wei Zen Wei, Wayne State University) was cloned from a spontaneous mammary tumor in BALB/c mice transgenic for the rat HER2/neu gene (BALB-HER2/neuT)[33] and was maintained by serial in vitro passages in CM.

All cells were grown at 37°C in a humidified 5% CO_2 incubator. BC cells were treated with IFN-γ (1–100 ng/mL), trastuzumab (10 μg/mL) and pertuzumab (10 μg/mL), or a combination of IFN-γ, trastuzumab, and pertuzumab for 1–6 days.

Cell proliferation assay
2,000–40,000 cells per well (depending on the growth of each cell line: TUBO, 2,000–3,000/well; JIMT-1, 10,000/well; HCC1419, 20,000/well; BT-474, ZR-75-30, SK-BR-3, and MDA-MB-453, 30,000–40,000/well) were plated in 12-well plates and treated with different treatment conditions as specified above for 5–6 days. Cells were then washed with PBS and stained with 0.5% crystal violet solution (prepared in 25% methanol) for 10 min. Stained cell colonies were washed with PBS and dried overnight, and images were obtained by a digital image scanner (HP 8300). Percentage colony area was determined using ImageJ v1.50i (https://imagej.nih.gov/ij/)[34] and the plugin "Colony Area."[35]

RNA interference (RNAi) transfections
Small interfering RNA (siRNA) SMARTpool: ON-TARGETplus CUL5 siRNA and STAT1 siRNA and SMARTpool: ON-TARGETplus non-targeting pool were purchased from Dharmacon (Lafayette, OH, USA), and siRNA transfection was performed following the manufacturer's protocol. Briefly, 300,000 cells were seeded in a six-well plate and grown for 24 h in complete medium to 75%–80% confluency. Cells were then transfected with no target control (siNT), CUL5, and STAT1 siRNA (30nM), using DharmaFECT transfection reagent. After 24 h, transfection media were removed and replaced with CM. Cells were then passaged and used for various designated treatments. Cells were harvested and total protein was extracted from transfected cells, following the same protocol as described below. Western blot was performed to compare protein expression between non-target and target siRNA-transfected cells.

Lentivirus transduction
Lentivirus containing shCUL5 (sc-37575-V) and shScramble (sc-108080) were obtained from Santa Cruz Biotechnology (Santa Cruz, CA, USA). Transduction was performed according to the manufacturer's protocol. Briefly, TUBO cells were infected with shScramble or shCUL5 lentivirus in the presence of 5 μg/mL Polybrene (sc-134220) for 24 h. The culture medium was removed and replaced with CM without Polybrene for 24–48 h. Following transduction, cells were selected by culturing in 2 μg/mL puromycin containing CM.

Senescence-associated β-galactosidase (SA-β-gal) activity at pH 6
Cells were treated and washed twice in PBS, fixed in 3% formaldehyde for 15 min, and rinsed with PBS. Cells were then incubated overnight

at 37°C (without CO_2) with freshly prepared SA-β-gal staining solution (Millipore) as per the manufacturer's instructions. The percentage of SA-β-gal-positive (blue) cells in each sample was determined using a bright-field microscope (EVOS Core XL, Bothell, WA, USA; ×40/2,048 × 1,536-pixel resolution, 3.2 μm/pixel; 3.1 megapixel [MP] color/captured images: color TIFF, PNG, JPG, or BMP, 2,048 × 1,536 pixels)

Mouse models

Female BALB/c mice at 6–8 weeks of age were purchased from Charles River Laboratories. C.129S7(B6)-$Ifng^{tm1Ts}$/J (IFN-γ^{KO}) mice were purchased from Jackson Laboratory. BALB-HER2/neu transgenic mice were a kind gift from Dr. Shari Pilon-Thomas (H. Lee Moffitt Cancer Center and Research Institute). Mice were housed at the Animal Research Facility of the H. Lee Moffitt Cancer Center and Research Institute. All mouse experiments were reviewed and approved by the Institutional Animal Care and Use Committee at the University of South Florida (no. A4100-01). All experiments were performed in accordance with the US Public Health Service policy and National Research Council guidelines.

IFN-γ treatment in combination with anti-HER2 antibody *in vivo*

3×10^4 TUBO cells were inoculated into the mammary fat pads of female BALB/c mice. On day 12 when mice had a palpable tumor, they were randomized into the following groups: (1) untreated, (2) IFN-γ, (3) anti-neu antibody, and (4) combination therapy with IFN-γ and anti-neu antibody. For monotherapy, mice received IFN-γ (5×10^5 IU/kg, three times weekly) and neu antibodies (clone 7.16.4, 50 μg and 7.9.5, 50 μg, once weekly) starting on day 12. For combination treatments, group no. 4 received anti-neu antibody on day 12; 4 days later, mice received IFN-γ. Mice were monitored for tumor growth twice a week, and tumor volumes were measured using the formula (length × width)2/2 = mm^3.

BALB-neuT mice experiment and MRI imaging

BALB-neuT mice (breeding pair was a kind gift from Dr. Federica Cavallo, University of Torino) at 8 weeks of age received intramammary gland delivery of class II neu peptide-pulsed DC1 vaccine (neu-DC1) (1×10^6 cells/mouse, once weekly for 6 weeks) guided by ultrasound. Untreated mice received sterile PBS injection in the mammary gland. The neu-DC1 vaccine was prepared as previously described.[20] The development of spontaneous tumor growth in the mammary glands of mice was monitored by magnetic resonance imaging (MRI). All mice were imaged on a 7-Tesla horizontal MRI scanner (Bruker Biospin, BioSpec AV3HD) using a 35-mm Litzcage coil (Doty Scientific). Mice were anesthetized in an induction chamber with 2% isoflurane delivered in 1.5 L/min oxygen and transferred for imaging. The same ventilation was maintained through a nose cone to maintain respiration at a range of 40–60 breaths per minute while imaging. The body core temperature was monitored and maintained at 37°C using a MR-compatible small rodent heater system (SAII, SA Instruments, Stony Brook, NY, USA). Anatomical T2-weighted coronal images were acquired with a TurboRARE sequence with echo time/repetition time (TR/TE) = 4,513/38 ms, field of view

(FOV) = 75 × 35 mm^2, image size of 512 × 256 pixels, slice thickness of 1.2 mm, and 19 slices. At 16 weeks of age, untreated and neu-DC1-vaccinated BALB-HER2/neuT mice were sacrificed and mammary tumor glands were collected for western blot and IHC staining. Spleens were collected for functional assays.

In another set of experiments, IFN-γ^{KO} mice were inoculated with TUBO cells (2.5×10^5 cells/100 μL/mouse) subcutaneously. When mice developed palpable tumors, a neu-DC1 vaccine (1×10^6 cells/mouse) was injected intratumorally once a week for 6 weeks. Untreated TUBO cell-bearing IFN-γ^{KO} mice received intratumoral PBS injections. Tumor growth was measured and recorded.

IFN-γ quantification by ELISA

To examine the anti-neu Th1 immune response generated by a neu-DC1 vaccine, spleens of untreated and neu-DC1-vaccinated BALB-HER2/neuT mice were collected, and splenocytes were prepared as previously described.[20] Splenocytes (2×10^6 cells) were stimulated with or without multi-epitope class II rat HER2/neu peptides P5, P435, and P1209 (2 μg/mL) individually for 72 h. After the incubation, culture supernatants were collected and centrifuged at 1,000 rpm for 5 min to remove floating cells. IFN-γ secretion was measured in the culture supernatants using a commercially available mouse IFN-γ Quantikine ELISA kit (R&D Systems, catalog no. SMIF00) according to the manufacturer's recommendations.

Tumor-inducing potential of CUL5 knocked out TUBO cell line

IFN-γ^{KO} BALB/c mice and wild-type BALB/c mice were injected with shScramble or shCUL5 TUBO cells (3×10^4 cells/mouse) into the mammary fat pad. Mice were monitored for tumor growth twice a week. Tumor volume was recorded and calculated. Mice were sacrificed at week 5, tumors were collected, and IHC staining was performed for neu and Ki-67 proteins.

Pretreatment of human BC cell line with IFN-γ and tumor growth in NSG mice

JIMT-1 cells, which are clinically resistant to trastuzumab, were treated with IFN-γ (10 ng/mL) or T+P (5 μg/mL each) for 48 h *in vitro*. Following treatment, cells were collected and examined for viability. 3×10^6 viable JIMT-1 cells from the untreated control group, the IFN-γ-treated group, and the T+P-treated group were re-suspended in sterile PBS and mixed with an equal volume of Cultrex basement membrane extract (BME). Next, prepared cells were injected in NSG mice subcutaneously. Mice were monitored for tumor growth and measured twice a week after tumors were palpable.

IHC

For IHC analysis of neu, Ki-67, and CUL5 expression, the collected tumor tissues were fixed in formalin and embedded in paraffin. 5-μm sections of paraffin-embedded tumor tissue blocks were placed onto glass slides coated with poly-L-lysine. Sections were deparaffinized by two washes in xylene for 5 min each and rehydrated by washing in graded alcohol for 5 min, followed by a final wash in water. Antigen retrieval was done using Tris-EDTA buffer, and endogenous

peroxidase activity was blocked by a 30-min incubation with 3% hydrogen peroxidase. Sections were blocked with 10% normal goat serum in Tris-buffered saline (TBS) to prevent non-specific binding of antibodies. Sections were then incubated overnight with primary anti-rabbit neu, anti-rabbit Ki-67, and anti-rabbit CUL5 antibodies. After washing, sections were incubated with horseradish peroxidase (HRP) conjugated with goat anti-rabbit secondary antibody for 1 h at 37°C. Antibody binding was detected a using 3,3′-diaminobenzidine (DAB) detection system and counterstained with hematoxylin solution. Slides were scanned with a Leica Aperio AT2 scanner (Leica Biosystems, Vista, CA, USA) at the Microscopy Core Facility of the H. Lee Moffitt Cancer Center and Research Institute.

Western blot analysis

Following various treatments, cell lysates were prepared by incubating in radioimmunoprecipitation assay (RIPA) buffer (Millipore) containing protease inhibitor cocktail (Sigma-Aldrich, St. Louis, MO, USA) and phosphatase inhibitor (Millipore) for 20 min at 4°C. Following incubation, lysates were centrifuged at $14,000 \times g$ for 20 min at 4°C. Protein concentration was measured using a Bradford protein assay (Bio-Rad, Hercules, CA, USA). Quantified proteins were resolved on 4%–12% SDS-PAGE (GenScript, Piscataway, NJ, USA), electroblotted onto polyvinylidene fluoride (PVDF) membranes (Millipore) using an eBlot L1 wet transfer system (GenScript, Piscataway, NJ, USA), and immunoblotted with the following primary antibodies: p16INK4a (sc-9968), CUL5 (sc-373822), and Cdc37 (sc-13129) (Santa Cruz Biotechnology, Santa Cruz, CA, USA); and HER2 (2165S), β-actin (4967S), HSP90 (4877S), Stat1 (14994S), anti-AKT (4691), anti-pS473-AKT (4060), and phosphorylated (p-)Stat1 (9167S) (Cell Signaling Technologies, Danvers, MA, USA). After washing, membranes were incubated with HRP-conjugated secondary antibody (Bio-Rad, Hercules, CA, USA). Protein expression was detected using the enhanced chemiluminescence (ECL) western blot detection system and was quantified by using the ECL western blot detection system and Image Reader LAS-1000 Lite version 1.0 software (Fuji). Quantification of western blots was performed using ImageJ software (https://imagej.nih.gov/ij/).

IP and western blotting analyses from cell lysate

IP was performed to investigate protein-protein interaction after Th1 cytokine treatment in human HER2^{pos} BC cells, as described elsewhere,[36] with modifications. Briefly, cells were treated with 20 ng/mL IFN-γ for 24 or 96 h, and total protein was extracted from cell lysates in IP lysis buffer (Pierce). For IP, 1 mg of cell lysate total protein and antibody (mouse anti-HER2 antibody, dilution 1:100; 2–4 μg of anti-Cdc37 antibody, according to the manufacturer's instructions) were allowed to conjugate overnight at 4°C on a rotating mixer. On the next day, 50 μL of protein G agarose beads in 100 μL of resin slurry (Pierce) was added to the antigen-antibody complex and was incubated at room temperature for 2 h, with gentle mixing. Beads were washed in 0.5 mL of IP buffer (Pierce), centrifuged for 3 min at $2,500 \times g$, and supernatants were discarded. For elution of the immune complex, 50 μL of elution buffer (Pierce) was added to the beads and supernatant was collected after centrifugation at $2,500 \times g$ for 3 min. Elution was performed twice, and two supernatant frac-

tions were combined. Samples were analyzed by western blotting, as described above, and were probed with the following antibodies: HER2 (2165S), ubiquitin (3933S), CUL5 (sc-373822), Cdc37 (sc-13129), and HSP90 (4877S) (Cell Signaling Technology).

Quantitative PCR (qPCR)

Total RNA was isolated using a Direct-zol RNA miniprep kit (Zymo Research), and 1 μg of each RNA sample was reverse transcribed into complementary DNA (cDNA) in a 20-μL reaction using an iScript cDNA synthesis kit (Bio-Rad). The reverse transcription reaction was performed using the thermocycler protocol as follows: 25°C for 5 min (priming), 46°C for 20 min (reverse transcription), 95°C for 1 min (reverse transcriptase [RT] inactivation). qPCR was performed using a TaqMan qPCR kit (TaqMan fast advanced master mix, 4444556). Each PCR amplification was carried out in a 20-μL volume containing 100 ng of cDNA and 0.25 μM of each of the specific forward and reverse primers for human CUL5 (Hs00967483_m1), human HER2 (Hs01001580_m1) and human GAPDH (Hs02758991_g1). PCR conditions used for all reactions are as follows: 94°C for 3 min, 30 cycles at 94°C (denaturation) for 30 s, 60°C for 30 s (annealing), and 72°C for 30 s (extension); the final extension was performed at 72°C for 5 min. Relative gene expression was calculated from the ratio of sample and control (cortex) according to Pfaffl.[37]

Immunofluorescence

For immunofluorescence experiments, 100,000 cells were seeded into six-well tissue culture plates (Corning Life Sciences) containing 13-mm-diameter round glass coverslips. After the appropriate treatments, cells were fixed with 4% paraformaldehyde for 15 min at room temperature. After being washed three times with PBS, cells were permeabilized by incubation with 0.2% Triton X-100 for 10 min. Cells were then washed with PBS, blocked with 5% BSA for 1 h at 4°C, and incubated with primary anti-rabbit HER2/ErbB2 antibody (1:500 dilution) (2165S; Cell Signaling Technology) and anti-mouse Cdc37 (1:50 dilution) (sc-13129; Santa Cruz Biotechnology, Santa Cruz, CA) in 1% BSA overnight at 4°C. Subsequently, cells were washed three times with PBS and incubated with Alexa Fluor 594-conjugated goat anti-rabbit secondary antibody (1:5,000 dilution) (Cell Signaling) and fluorescein isothiocyanate (FITC)-conjugated goat anti-mouse secondary antibody (1:5,000 dilution) (Jackson Laboratory) in 1% BSA for 1 h at room temperature in the dark.

Following three PBS washes, coverslips were mounted onto sterile glass slides using Vectashield antifade mounting medium with DAPI (Vector Laboratories). The slides were allowed to cure overnight at 4°C in the dark and sealed with clear nail varnish. Cells were analyzed and imaged by using a Zeiss ApoTome.2 fluorescence microscope (Carl Zeiss, Thornwood, NY, USA). In some experiments, immunofluorescence images were captured using the Leica SP8 confocal microscope.

Cell cycle analysis by flow cytometry

For cell cycle analysis, shScramble and shCUL5 TUBO cells were harvested, washed twice with PBS, and fixed with 70% ethanol overnight at 4°C. Next, cells were washed with PBS, incubated with RNase A for

30 min at room temperature, and stained with propidium iodide (PI) (50 μg/mL) for 1 h at room temperature in the dark. The stained cells were analyzed for cell cycle distribution by flow cytometry.

Oncomine database analysis

The Oncomine database (https://www.oncomine.org/resource/login.html), a web-based microarray database, was used to analyze the transcription level of CUL5 in different cancer types.[38,39] It is an integrated platform for data mining. 18,000 cancer gene expression experiments are included in the release of Oncomine 3.0. CUL5 gene expression in BC tissue was queried and compared that with normal tissue by using a Student's t test. The parameters included fold change ≥2, p value ≤1E−4, and gene rank ≥top 10%.

cBioportal analysis

cBioPortal (https://www.cbioportal.org/),[40,41] which is an open access resource for cancer genomic data, was used to query for the relationship between CUL5, cdc37, and HSP90AB1 alterations and BC OS. A total of 1,054 samples were analyzed from two studies: the MBC project (MBC, 237 cases) and breast TCGA 2015 (invasive breast carcinoma, 817 cases).

Bioinformatics analysis by bc-GenExMiner v4.2

bc-GenExMiner v4.2,[42,43] a mining tool of 36 published annotated genomics data (total of 5,696 patients), was used to conduct CUL5 survival analysis in different molecular subtypes, including HER2-E, ER^{pos}, HER2^{neg}, and ER^{neg}. The relevance of CUL5 expression and prognosis was analyzed through univariate Cox analysis and Kaplan-Meier curve analysis. 40% was set as the cutoff to define high and low expression of CUL5.

Statistical analysis

All data are shown as the mean ± SEM, and statistical analyses were performed with Prism 7.0. To determine whether samples were normally distributed, D'Agostino and Pearson (n > 7) or Shapiro-Wilk (n < 7) tests were performed. Differences between mean values of two groups were analyzed using an unpaired or paired two-tailed t test or two-tailed Mann-Whitney or Wilcoxon test. Mean differences of more than two groups were analyzed using one-way analysis of variance (ANOVA) with Sidak's multiple comparisons post hoc test or a Friedman's test with a Dunn's multiple comparisons post hoc test. Differences in scratching time-course experiments were analyzed with two-way ANOVA and a Sidak's multiple comparisons post hoc test. Differences were considered significant for p <0.05. Exact p values and their definition and the number of replicates are given in the respective figure legends.

SUPPLEMENTAL INFORMATION

Supplemental Information can be found online at https://doi.org/10.1016/j.ymthe.2020.12.037.

AUTHOR CONTRIBUTIONS

Y.J. and B.J.C. conceived and designed experiments. Y.J., G.R., A.B., K.N.K., D.W., and C.S. performed experiments. Y.J., K.N.K., C.S., G.R., Y.-Z.C., and B.J.C. analyzed data and contributed to data analysis. K.N.K. and B.J.C. supervised the work. Y.J., K.N.K., A.B., and B.J.C. wrote the manuscript, and H.Z., M.I.G., Q.M., Z.T., H.H., H.S., J.R.C.-G., and G.K. edited the manuscript.

DECLARATION OF INTERESTS

B.J.C. and G.K. have a patent application filed for intellectual property on a human version of DC1.

REFERENCES

1. Broglio, K.R., Quintana, M., Foster, M., Olinger, M., McGlothlin, A., Berry, S.M., Boileau, J.F., Brezden-Masley, C., Chia, S., Dent, S., et al. (2016). Association of pathologic complete response to neoadjuvant therapy in HER2-positive breast cancer with long-term outcomes: a meta-analysis. JAMA Oncol. 2, 751–760.

2. Cortazar, P., Zhang, L., Untch, M., Mehta, K., Costantino, J.P., Wolmark, N., Bonnefoi, H., Cameron, D., Gianni, L., Valagussa, P., et al. (2014). Pathological complete response and long-term clinical benefit in breast cancer: the CTNeoBC pooled analysis. Lancet 384, 164–172.

3. Freudenberg, J.A., Wang, Q., Katsumata, M., Drebin, J., Nagatomo, I., and Greene, M.I. (2009). The role of HER2 in early breast cancer metastasis and the origins of resistance to HER2-targeted therapies. Exp. Mol. Pathol. 87, 1–11.

4. Witzel, I., Oliveira-Ferrer, L., Pantel, K., Müller, V., and Wikman, H. (2016). Breast cancer brain metastases: biology and new clinical perspectives. Breast Cancer Res. 18, 8.

5. Darlix, A., Louvel, G., Fraisse, J., Jacot, W., Brain, E., Debled, M., Mouret-Reynier, M.A., Goncalves, A., Dalenc, F., Delaloge, S., et al. (2019). Impact of breast cancer molecular subtypes on the incidence, kinetics and prognosis of central nervous system metastases in a large multicentre real-life cohort. Br. J. Cancer 121, 991–1000.

6. Mittendorf, E.A., Clifton, G.T., Holmes, J.P., Schneble, E., van Echo, D., Ponniah, S., and Peoples, G.E. (2014). Final report of the phase I/II clinical trial of the E75 (nelipepimut-S) vaccine with booster inoculations to prevent disease recurrence in high-risk breast cancer patients. Ann. Oncol. 25, 1735–1742.

7. Andre, F., Dieci, M.V., Dubsky, P., Sotiriou, C., Curigliano, G., Denkert, C., and Loi, S. (2013). Molecular pathways: involvement of immune pathways in the therapeutic response and outcome in breast cancer. Clin. Cancer Res. 19, 28–33.

8. Datta, J., Berk, E., Xu, S., Fitzpatrick, E., Rosemblit, C., Lowenfeld, L., Goodman, N., Lewis, D.A., Zhang, P.J., Fisher, C., et al. (2015). Anti-HER2 CD4$^+$ T-helper type 1 response is a novel immune correlate to pathologic response following neoadjuvant therapy in HER2-positive breast cancer. Breast Cancer Res. 17, 71.

9. Datta, J., Fracol, M., McMillan, M.T., Berk, E., Xu, S., Goodman, N., Lewis, D.A., DeMichele, A., and Czerniecki, B.J. (2016). Association of depressed anti-HER2 T-helper type 1 response with recurrence in patients with completely treated HER2-positive breast cancer: role for immune monitoring. JAMA Oncol. 2, 242–246.

10. Namjoshi, P., Showalter, L., Czerniecki, B.J., and Koski, G.K. (2019). T-helper 1-type cytokines induce apoptosis and loss of HER-family oncodriver expression in murine and human breast cancer cells. Oncotarget 10, 6006–6020.

11. Rosemblit, C., Datta, J., Lowenfeld, L., Xu, S., Basu, A., Kodumudi, K., Wiener, D., and Czerniecki, B.J. (2018). Oncodriver inhibition and CD4+ Th1 cytokines cooperate through Stat1 activation to induce tumor senescence and apoptosis in HER2+ and triple negative breast cancer: implications for combining immune and targeted therapies. Oncotarget 9, 23058–23077.

12. Nagai, Y., Tsuchiya, H., Runkle, E.A., Young, P.D., Ji, M.Q., Norton, L., Drebin, J.A., Zhang, H., and Greene, M.I. (2015). Disabling of the erbB pathway followed by IFN-γ modifies phenotype and enhances genotoxic eradication of breast tumors. Cell Rep. 12, 2049–2059.

13. Pearl, L.H. (2005). Hsp90 and Cdc37—a chaperone cancer conspiracy. Curr. Opin. Genet. Dev. 15, 55–61.

14. Luque-Cabal, M., García-Teijido, P., Fernández-Pérez, Y., Sánchez-Lorenzo, L., and Palacio-Vázquez, I. (2016). Mechanisms behind the resistance to trastuzumab in HER2-amplified breast cancer and strategies to overcome it. Clin. Med. Insights Oncol. 10 (Suppl 1), 21–30.

15. de Melo Gagliato, D., Jardim, D.L., Marchesi, M.S., and Hortobagyi, G.N. (2016). Mechanisms of resistance and sensitivity to anti-HER2 therapies in HER2+ breast cancer. Oncotarget 7, 64431–64446.

16. Costa, R.L.B., and Czerniecki, B.J. (2020). Clinical development of immunotherapies for HER2+ breast cancer: a review of HER2-directed monoclonal antibodies and beyond. NPJ Breast Cancer 6, 10.

17. Geyer, C.E., Forster, J., Lindquist, D., Chan, S., Romieu, C.G., Pienkowski, T., Jagiello-Gruszfeld, A., Crown, J., Chan, A., Kaufman, B., et al. (2006). Lapatinib plus capecitabine for HER2-positive advanced breast cancer. N. Engl. J. Med. 355, 2733–2743.

18. Verma, S., Miles, D., Gianni, L., Krop, I.E., Welslau, M., Baselga, J., Pegram, M., Oh, D.Y., Diéras, V., Guardino, E., et al.; EMILIA Study Group (2012). Trastuzumab emtansine for HER2-positive advanced breast cancer. N. Engl. J. Med. 367, 1783–1791.

19. Modi, S., Saura, C., Yamashita, T., Park, Y.H., Kim, S.B., Tamura, K., Andre, F., Iwata, H., Ito, Y., Tsurutani, J., et al. (2020). Trastuzumab deruxtecan in previously treated HER2-positive breast cancer. N. Engl. J. Med. 382, 610–621.

20. Kodumudi, K.N., Ramamoorthi, G., Snyder, C., Basu, A., Jia, Y., Awshah, S., Beyer, A.P., Wiener, D., Lam, L., Zhang, H., et al. (2019). Sequential anti-PD1 therapy following dendritic cell vaccination improves survival in a HER2 mammary carcinoma model and identifies a critical role for CD4 T cells in mediating the response. Front. Immunol. 10, 1939.

21. Rolla, S., Nicoló, C., Malinarich, S., Orsini, M., Forni, G., Cavallo, F., and Ria, F. (2006). Distinct and non-overlapping T cell receptor repertoires expanded by DNA vaccination in wild-type and HER-2 transgenic BALB/c mice. J. Immunol. 177, 7626–7633.

22. Ahmad, A. (2019). Current updates on trastuzumab resistance in HER2 overexpressing breast cancers. Adv. Exp. Med. Biol. 1152, 217–228.

23. Vernieri, C., Milano, M., Brambilla, M., Mennitto, A., Maggi, C., Cona, M.S., Prisciandaro, M., Fabbroni, C., Celio, L., Mariani, G., et al. (2019). Resistance mechanisms to anti-HER2 therapies in HER2-positive breast cancer: Current knowledge, new research directions and therapeutic perspectives. Crit. Rev. Oncol. Hematol. 139, 53–66.

24. Gianni, L., Pienkowski, T., Im, Y.H., Roman, L., Tseng, L.M., Liu, M.C., Lluch, A., Staroslawska, E., de la Haba-Rodriguez, J., Im, S.A., et al. (2012). Efficacy and safety of neoadjuvant pertuzumab and trastuzumab in women with locally advanced, inflammatory, or early HER2-positive breast cancer (NeoSphere): a randomised multicentre, open-label, phase 2 trial. Lancet Oncol. 13, 25–32.

25. Nahta, R., Hung, M.C., and Esteva, F.J. (2004). The HER-2-targeting antibodies trastuzumab and pertuzumab synergistically inhibit the survival of breast cancer cells. Cancer Res. 64, 2343–2346.

26. Cuello, M., Ettenberg, S.A., Clark, A.S., Keane, M.M., Posner, R.H., Nau, M.M., Dennis, P.A., and Lipkowitz, S. (2001). Down-regulation of the erbB-2 receptor by trastuzumab (herceptin) enhances tumor necrosis factor-related apoptosis-inducing ligand-mediated apoptosis in breast and ovarian cancer cell lines that overexpress erbB-2. Cancer Res. 61, 4892–4900.

27. Nahta, R., Yu, D., Hung, M.C., Hortobagyi, G.N., and Esteva, F.J. (2006). Mechanisms of disease: understanding resistance to HER2-targeted therapy in human breast cancer. Nat. Clin. Pract. Oncol. 3, 269–280.

28. Salgado, R., Denkert, C., Campbell, C., Savas, P., Nuciforo, P., Aura, C., de Azambuja, E., Eidtmann, H., Ellis, C.E., Baselga, J., et al. (2015). Tumor-infiltrating lymphocytes and associations with pathological complete response and event-free survival in HER2-positive early-stage breast cancer treated with lapatinib and trastuzumab: a secondary analysis of the NeoALTTO trial. JAMA Oncol. 1, 448–454.

29. Denkert, C., von Minckwitz, G., Darb-Esfahani, S., Lederer, B., Heppner, B.I., Weber, K.E., Budczies, J., Huober, J., Klauschen, F., Furlanetto, J., et al. (2018). Tumour-infiltrating lymphocytes and prognosis in different subtypes of breast cancer: a pooled analysis of 3771 patients treated with neoadjuvant therapy. Lancet Oncol. 19, 40–50.

30. Rinnerthaler, G., Gampenrieder, S.P., and Greil, R. (2019). HER2 directed antibody-drug-conjugates beyond T-DM1 in breast cancer. Int. J. Mol. Sci. 20, 1115.

31. Dirix, L.Y., Takacs, I., Jerusalem, G., Nikolinakos, P., Arkenau, H.T., Forero-Torres, A., Boccia, R., Lippman, M.E., Somer, R., Smakal, M., et al. (2018). Avelumab, an anti-PD-L1 antibody, in patients with locally advanced or metastatic breast cancer: a phase 1b JAVELIN Solid Tumor study. Breast Cancer Res. Treat. 167, 671–686.

32. Agus, D.B., Akita, R.W., Fox, W.D., Lewis, G.D., Higgins, B., Pisacane, P.I., Lofgren, J.A., Tindell, C., Evans, D.P., Maiese, K., et al. (2002). Targeting ligand-activated ErbB2 signaling inhibits breast and prostate tumor growth. Cancer Cell 2, 127–137.

33. Rovero, S., Amici, A., Di Carlo, E., Bei, R., Nanni, P., Quaglino, E., Porcedda, P., Boggio, K., Smorlesi, A., Lollini, P.L., et al. (2000). DNA vaccination against rat her-2/Neu p185 more effectively inhibits carcinogenesis than transplantable carcinomas in transgenic BALB/c mice. J. Immunol. 165, 5133–5142.

34. Schneider, C.A., Rasband, W.S., and Eliceiri, K.W. (2012). NIH Image to ImageJ: 25 years of image analysis. Nat. Methods 9, 671–675.

35. Guzmán, C., Bagga, M., Kaur, A., Westermarck, J., and Abankwa, D. (2014). ColonyArea: an ImageJ plugin to automatically quantify colony formation in clonogenic assays. PLoS ONE 9, e92444.

36. Samant, R.S., Clarke, P.A., and Workman, P. (2014). E3 ubiquitin ligase Cullin-5 modulates multiple molecular and cellular responses to heat shock protein 90 inhibition in human cancer cells. Proc. Natl. Acad. Sci. USA 111, 6834–6839.

37. Pfaffl, M.W., Tichopad, A., Prgomet, C., and Neuvians, T.P. (2004). Determination of stable housekeeping genes, differentially regulated target genes and sample integrity: BestKeeper—Excel-based tool using pair-wise correlations. Biotechnol. Lett. 26, 509–515.

38. Rhodes, D.R., Kalyana-Sundaram, S., Mahavisno, V., Varambally, R., Yu, J., Briggs, B.B., Barrette, T.R., Anstet, M.J., Kincead-Beal, C., Kulkarni, P., et al. (2007). Oncomine 3.0: genes, pathways, and networks in a collection of 18,000 cancer gene expression profiles. Neoplasia 9, 166–180.

39. Rhodes, D.R., Yu, J., Shanker, K., Deshpande, N., Varambally, R., Ghosh, D., Barrette, T., Pandey, A., and Chinnaiyan, A.M. (2004). ONCOMINE: a cancer microarray database and integrated data-mining platform. Neoplasia 6, 1–6.

40. Cerami, E., Gao, J., Dogrusoz, U., Gross, B.E., Sumer, S.O., Aksoy, B.A., Jacobsen, A., Byrne, C.J., Heuer, M.L., Larsson, E., et al. (2012). The cBio cancer genomics portal: an open platform for exploring multidimensional cancer genomics data. Cancer Discov. 2, 401–404.

41. Gao, J., Aksoy, B.A., Dogrusoz, U., Dresdner, G., Gross, B., Sumer, S.O., Sun, Y., Jacobsen, A., Sinha, R., Larsson, E., et al. (2013). Integrative analysis of complex cancer genomics and clinical profiles using the cBioPortal. Sci. Signal. 6, pl1.

42. Jézéquel, P., Frénel, J.S., Campion, L., Guérin-Charbonnel, C., Gouraud, W., Ricolleau, G., and Campone, M. (2013). bc-GenExMiner 3.0: new mining module computes breast cancer gene expression correlation analyses. Database (Oxford) 2013, bas060.

43. Jézéquel, P., Campone, M., Gouraud, W., Guérin-Charbonnel, C., Leux, C., Ricolleau, G., and Campion, L. (2012). bc-GenExMiner: an easy-to-use online platform for gene prognostic analyses in breast cancer. Breast Cancer Res. Treat. 131, 765–775.